

## REVIEW

[View Article Online](#)  
[View Journal](#) | [View Issue](#)Cite this: *Nanoscale Adv.*, 2024, 6, 3513

## MXene-based composites in smart wound healing and dressings

Atefeh Zarepour,<sup>a</sup> Nesa Rafati,<sup>b</sup> Arezoo Khosravi,<sup>\*c</sup> Navid Rabiee,<sup>id d</sup>  
Siavash Irvani<sup>id \*e</sup> and Ali Zarrabi<sup>id \*fg</sup>

MXenes, a class of two-dimensional materials, exhibit considerable potential in wound healing and dressing applications due to their distinctive attributes, including biocompatibility, expansive specific surface area, hydrophilicity, excellent electrical conductivity, unique mechanical properties, facile surface functionalization, and tunable band gaps. These materials serve as a foundation for the development of advanced wound healing materials, offering multifunctional nanoplatforms with theranostic capabilities. Key advantages of MXene-based materials in wound healing and dressings encompass potent antibacterial properties, hemostatic potential, pro-proliferative attributes, photothermal effects, and facilitation of cell growth. So far, different types of MXene-based materials have been introduced with improved features for wound healing and dressing applications. This review covers the recent advancements in MXene-based wound healing and dressings, with a focus on their contributions to tissue regeneration, infection control, anti-inflammation, photothermal effects, and targeted therapeutic delivery. We also discussed the constraints and prospects for the future application of these nanocomposites in the context of wound healing/dressings.

Received 22nd March 2024

Accepted 20th May 2024

DOI: 10.1039/d4na00239c

[rsc.li/nanoscale-advances](https://rsc.li/nanoscale-advances)

## 1. Introduction

Wound healing is a complex biological process that involves several stages, including inflammation, proliferation, and remodeling. The use of wound dressings is a critical aspect of wound management, as they facilitate the healing process by protecting the wound from external contaminants, providing a moist environment for cell growth and migration, and promoting tissue regeneration. Traditional wound dressings such as gauze and bandages have limited efficacy in promoting wound healing, particularly in chronic and complex wounds. Consequently, researchers have been exploring the use of novel materials in wound dressings, including MXene-based composites.<sup>1,2</sup>

MXenes are a class of two-dimensional (2D) materials composed of transition metal carbides, nitrides, or carbonitrides with a general formula of  $M_{n+1}X_nT_x$  ( $n = 1-4$ ), where M represents transition metals, X is carbon and/or nitrogen, and T stands for surface termination groups ( $-OH$ ,  $-F$ ,  $-O$  or  $-Cl$ ). They can be produced using either top-down techniques (various etching methods) or bottom-up methods (such as plasma-enhanced pulsed laser deposition, chemical vapor deposition, and template approaches).<sup>3,4</sup> They were first discovered in 2011 by researchers at Drexel University and have since garnered significant attention owing to their exceptional physicochemical properties, such as high conductivity, excellent mechanical strength, and biocompatibility. MXenes have been explored in various applications, including energy storage, catalysis, and sensing. More recently, researchers have begun to investigate their potential in biomedical applications, particularly wound healing.<sup>5,6</sup>

MXene-based composites have shown promise in wound healing applications because of their multifunctionality and easy surface functionalization capabilities. These materials can be engineered to possess specific properties such as high porosity, biodegradability, and antimicrobial activity. The incorporation of MXenes into wound dressings can enhance the wound healing process by promoting cell migration, proliferation, and differentiation. In addition, MXenes can modulate the inflammatory response, which is a critical aspect of the wound healing process. The first MXene-based composite wound dressing was reported by researchers at Drexel University. The

<sup>a</sup>Department of Research Analytics, Saveetha Dental College and Hospitals, Saveetha Institute of Medical and Technical Sciences, Saveetha University, Chennai, 600 077, India

<sup>b</sup>Department of Nanobiotechnology, Faculty of Biological Science, Tarbiat Modares University, Tehran, Iran

<sup>c</sup>Department of Genetics and Bioengineering, Faculty of Engineering and Natural Sciences, Istanbul Okan University, Istanbul 34959, Turkey. E-mail: arezoo.khosravi@okan.edu.tr

<sup>d</sup>Centre for Molecular Medicine and Innovative Therapeutics, Murdoch University, Perth, WA 6150, Australia

<sup>e</sup>Independent Researcher, W Nazar ST, Boostan Ave, Isfahan, Iran. E-mail: siavashira@gmail.com

<sup>f</sup>Department of Biomedical Engineering, Faculty of Engineering and Natural Sciences, Istinye University, Istanbul 34396, Turkey. E-mail: ali.zarrabi@istinye.edu.tr

<sup>g</sup>Graduate School of Biotechnology and Bioengineering, Yuan Ze University, Taoyuan 320315, Taiwan. E-mail: alizarrabi@gmail.com

dressing was composed of MXene nanosheets and chitosan, a biopolymer derived from chitin. Chitosan has been extensively studied for its wound healing properties, including its ability to promote cell growth, angiogenesis, and collagen synthesis. The MXene-chitosan composite dressing exhibited efficient antibacterial activities against both Gram-positive and Gram-negative bacteria, indicating its potential for preventing wound infections. The dressing also demonstrated good biocompatibility with human dermal fibroblasts, indicating its safety for use in wound healing applications.<sup>7–10</sup> Since the development of the MXene-chitosan composite dressing, several other MXene-based composite dressings have been reported.<sup>11–13</sup>

MXene-based composites have also been explored in the development of other wound healing applications, including tissue engineering (TE) scaffolds. Overall, TE involves the use of biomaterials to create scaffolds that can support the growth and regeneration of new tissue. MXenes have been investigated as potential scaffold materials with high porosity and mechanical strength. MXene-based scaffolds have shown promise in promoting tissue regeneration, particularly in bone and cartilage TE.<sup>14,15</sup> Besides, researchers reported MXene-based systems for smart wound dressing that could detect changes in pH, temperature, and humidity in the wound environment. The dressing was composed of MXene nanosheets and a hydrogel matrix that could absorb wound exudate. The MXene-based smart dressing showed excellent sensitivity and selectivity for detecting changes in the wound environment, indicating its potential for use in personalized wound care.<sup>10,16–18</sup>

As such, MXene-based composites represent a new frontier in wound healing and dressings and are likely to play key role in the development of novel wound care therapies in the future. However, further research is needed to fully explore their potential and optimize their properties for specific wound healing applications.<sup>19–21</sup> This review sets itself apart from other published papers by offering a comprehensive overview of the applications, benefits, and future prospects of MXene-based composites in wound healing and dressings. Moreover, this

review highlights the unique benefits of MXene composites, such as their conductivity, mechanical strength, biocompatibility, and antimicrobial properties, in the context of wound healing. By emphasizing the potential for tissue regeneration, accelerated healing, and infection prevention, this review offers a practical perspective on the clinical implications of using MXene-based materials in medical settings. In addition, the specific advantages of MXenes and their composites in wound dressings are deliberated, including their ability to facilitate controlled release of therapeutic agents and adapt to the wound surface for optimal coverage. Hopefully, by discussing these functionalities in detail, this review provides valuable insights into how MXene-based dressings can address current challenges in wound care and improve patient outcomes.

## 2. Properties of MXenes

MXenes possess fascinating properties derived from their complex bonding and electronic structures (Fig. 1).<sup>22</sup> The exceptional properties exhibited by MXenes are intimately connected to their unique chemical bonding and electronic structures. MXenes are primarily characterized by their strong metallic bonding within the transition metal (M) and carbon/nitrogen (X) layers, which results in excellent electronic conductivity. The surface functional groups, often terminated with elements such as oxygen (O), fluorine (F), or hydroxyl (OH), introduce polar covalent bonds, enhancing their hydrophilicity and rendering them suitable for various applications, including energy storage and conversion devices. These functional groups also influence the electronic structure by introducing localized states and controlling charge distribution. This interplay between metallic bonding, surface functionalization, and electronic structure leads to outstanding properties such as high electrical conductivity, impressive mechanical strength, and exceptional electrochemical performance, making MXenes a promising class of materials for a wide range of advanced technologies.<sup>23–26</sup>

MXenes have an exceptional electrical conductivity, which makes them valuable for applications in optoelectronics and

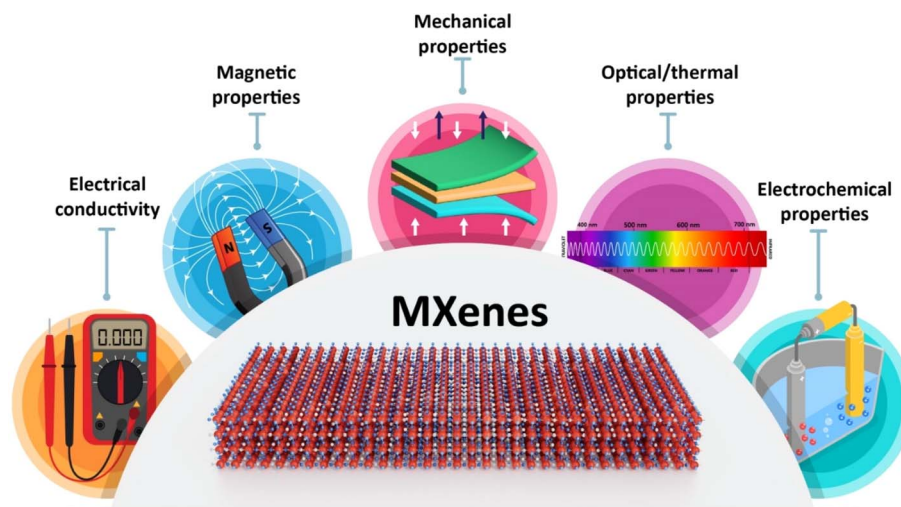


Fig. 1 MXenes and their important properties.



thermoelectrics.<sup>27</sup> MXenes have a high specific surface area and can be functionalized with various chemical groups, which can be applied for tuning their features.<sup>28</sup> In addition, these 2D materials have good hydrophilicity, metallic conductivity, and excellent mechanical properties, making them useful in various biomedical applications.<sup>29,30</sup>

The magnetic properties of MXenes have received less attention compared to their optical and electrical properties, creating a notable disparity between theoretical predictions and experimental validations. Most predicted magnetic MXenes involve magnetic transition metal elements such as Cr, V, Mn, Mo, Fe, Co, and Ni, either as constituents or in doped forms. Computational studies have extensively explored the quest for magnetic MXenes, predicting both ferromagnetic and antiferromagnetic phases. Density functional theory (DFT) calculations suggest that magnetic behavior can be altered intrinsically by varying the M-site metal and surface termination species and extrinsically by applying strains. However, there are limited experimental data on the magnetic properties of pristine MXenes due to limitations in material synthesis techniques.<sup>31,32</sup> MXenes with magnetic properties could be used in different applications, including cancer theranostics, spintronics, interference shielding, environmental applications, microwave absorption, and nanoelectronic devices.<sup>33–35</sup>

Notably, MXenes can be surface modified or functionalized with specific targeting moieties to deliver drugs/therapeutic agents to specific sites in the body, preventing or reducing the risk of side effects. Meanwhile, a variety of composites have been designed based on unique optical and thermal properties of MXenes/derivatives for non-invasive therapeutic strategies such as photothermal therapy. Indeed, their biocompatibility, hydrophilicity, excellent photothermal performance, high aspect ratios, and potential in absorption and conversion of different types of photons (ranging from UV to near infrared (NIR) light) introduce them as ideal candidates for photo-induced antimicrobial effects.<sup>36</sup> Besides, the above mentioned physicochemical and biological features of MXenes recommend them for tissue regeneration applications.<sup>14</sup> Organic or inorganic materials can be hybridized with MXenes, providing structures with multifunctionality and enhanced biocidal performances particularly for wound dressings or water purification;<sup>37</sup> several hybrid MXene-based platforms have been introduced for bacterial infection treatment as well as wound healing/dressings, with low cytotoxicity and high biocompatibility.<sup>38,39</sup>

### 3. MXenes against bacterial infections

MXenes have the potential to be a promising alternative to traditional antibiotics owing to their unique properties and potential applications in targeted drug delivery and non-invasive strategies against antibiotic-resistant pathogens.<sup>40,41</sup> MXenes employ three main mechanisms for exhibiting antibacterial activity: (a) inducing physical damage by sharp edges of MXene nanoflakes and direct mechanical destruction of bacterial cells,<sup>42</sup> (b) generation of reactive oxygen species (ROS), and (c) photothermal deactivation of bacteria (Fig. 2A). The

formation of ROS is due to their unique electronic properties, thus allowing them to interact with water molecules and generate hydrogen peroxide and hydroxyl radicals. The ROS produced by MXenes can cause oxidative damage to bacterial cells, leading to bacterial cell death.<sup>40,43</sup> However, it is critical to mention that ROS act as a double-edged sword in response to cells. Indeed, normal amounts of ROS have special roles in maintaining the hemostasis and functions of cells and regulating vascular constriction and relaxation, while increasing amounts of them lead to activation of immune system responses along with cellular death (*via* activation of apoptotic and necrotic pathways). So, it is critical to have a control on the amounts of ROS produced by the MXenes during the treatment process to prevent undesirable side effects.<sup>44</sup> It is revealed in the literature that different properties of MXenes such as their size, stability, dispersity, surface charge, and optical properties could affect their antibacterial activity (Fig. 2B). Indeed, their tunable optical properties, that has a relationship with their structure, enable them to act as a photothermal agent and convert the adsorbed UV-visible light into heat, that could directly affect bacteria *via* inducing DNA damage and protein degradation, producing reactive oxygen species (ROS) and enhancing the permeability of the bacterial membrane, all of which lead to bacterial death. The size of nanosheets also plays a crucial role in adsorption capacity, dispersibility, and the availability of sharp edges that could affect bacterial membranes, so smaller MXene flakes offer increased sharp edges, enhancing the likelihood of diffusion into cells and damaging cytoplasmic components, such as DNA. In addition, positively charged MXenes could attract bacteria due to the electrostatic interaction with the negative surface charge of bacteria. Therefore, negatively charged MXenes need modification to enhance their interactions with bacteria. Moreover, the presence of aggregation and sedimentation in MXene colloids decrease the contact area between the MXenes and bacteria, leading to reduced antibacterial properties. Besides, improving the stability of MXenes during their storage period, *via* removing oxygen from their solution or modifying their surface, could protect them from their antibacterial activity.<sup>45–48</sup>

Different research studies have been conducted until now in which antibacterial activity of MXenes was evaluated.<sup>49–52</sup> For instance, the antibacterial activity of the TiVCT<sub>x</sub> monolayer was evaluated against both *Escherichia coli* (*E. coli*) and *Bacillus subtilis* (*B. subtilis*) as Gram-negative and Gram-positive bacterial strains under NIR irradiation. This MXene showed excellent antibacterial activity *via* acting as a nano-knife that could affect bacteria *via* damaging their membrane from one side and exhibiting the photothermal conversion effect from the other side.<sup>53</sup>

A composite of 2,2,6,6-tetramethylpiperidiny-1-oxyl (TEMPO)-oxidized cellulose nanofibril (TOCN) and Ti<sub>3</sub>C<sub>2</sub>T<sub>x</sub> was fabricated and used as a type of electronic skin that showed ideal biocompatibility, electromagnetic shielding performance, and antibacterial properties (against *E. coli* and *Staphylococcus aureus* (*S. aureus*)). This antibacterial activity resulted from the physical interactions between bacteria and Ti<sub>3</sub>C<sub>2</sub>T<sub>x</sub> as well as its photothermal ability.<sup>54</sup> A composite of Ti<sub>3</sub>C<sub>2</sub>/CuFe<sub>2</sub>O<sub>4</sub> also exhibited antibacterial activity against different types of



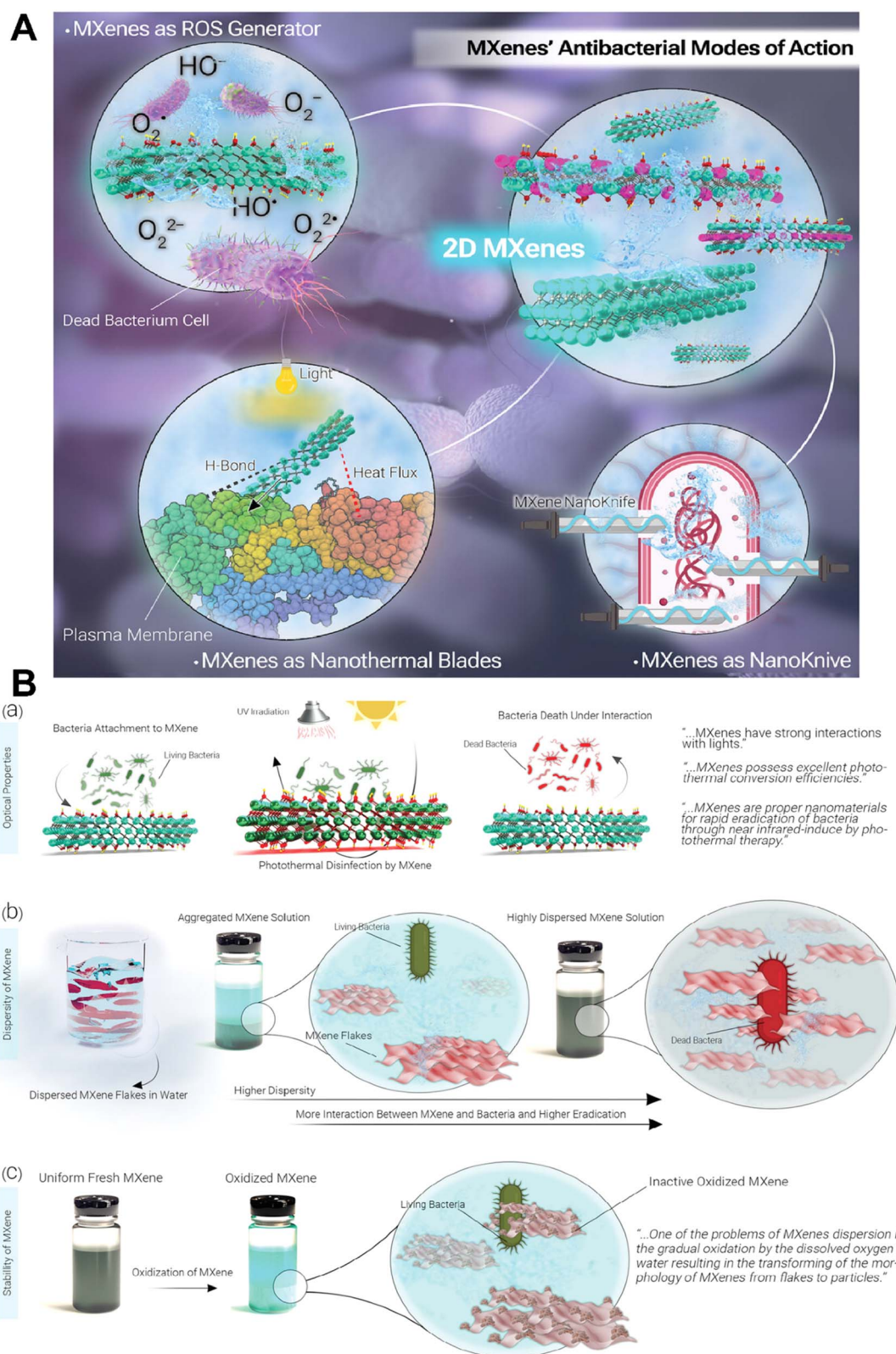
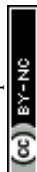


Fig. 2 Antibacterial activity of MXenes. (A) Schematic representation of different mechanisms of the antibacterial activity of MXenes. (B) Effect of different properties of MXenes on their antibacterial activity. Reprinted with permission from ref. 45. Copyright 2023, Wiley.



bacterial strains *via* producing ROS inside bacteria that affected bacterial proteins and DNA, from one side, and reducing the permeability of the bacterial membrane *via* interaction between the positively charged metals and the bacterial membrane.<sup>55</sup>

The potential side effects of using MXenes for antibacterial therapy are still under active research, and more studies are required to fully understand the safety and toxicity of these materials.<sup>42</sup> So far, most of the studies on MXenes and their antibacterial properties have focused on their short-term effects and mechanisms of action. There is currently no information available on the long-term consequences of using MXenes for antibacterial therapy. Thus, future explorations should be focused on investigation of the long-term effects of using MXenes for antibacterial therapy.<sup>41,56,57</sup> Meanwhile, the inevitable release of MXenes into the natural environment because of their increasing fabrication and application may cause negative effects on human health and the ecosystem. Thus, it is vital to gently consider the environmental impact of MXenes and their potential long-term effects on human health before widespread applications.<sup>42,48</sup>

## 4. Advanced wound dressing/healing applications

Currently, numerous researchers have made significant advancements in developing novel composite materials for wound dressings that incorporate MXene nanomaterials.<sup>6,58,59</sup> These materials could enhance the exceptional properties of MXenes, as discussed earlier, to effectively sterilize wounds, enable sustained drug release, and actively regulate cytokines within skin wounds.<sup>60</sup> This development greatly expands the ideas and approaches that could be used for treating chronic wounds. In this section, we provide a comprehensive overview of MXene composites, categorizing them into five distinct groups based on their underlying advanced applications in wound healing.

### 4.1 Delivery carriers

The unique characteristics of MXenes make them attractive candidates for controlled and targeted drug delivery purposes.<sup>61</sup> The high specific surface area of MXenes provides a huge space for loading and encapsulating therapeutic molecules, such as drugs, proteins, and nucleic acids, *via* adsorption or bonding, that ensure their stability during storage and transportation and offer their controlled release.<sup>62</sup> The release kinetics can be modulated by adjusting the surface functionalization, interlayer spacing, or by incorporating stimuli-responsive elements into the MXene structure.<sup>63</sup> For example, pH responsive MXenes can release the cargo in response to the acidic environment of specific target sites, such as tumors or inflamed tissues. This could enhance therapeutic efficacy while minimizing off-target side effects.<sup>64</sup> MXenes have also demonstrated excellent biocompatibility and low cytotoxicity, which are crucial for an ideal delivery carrier.<sup>65</sup>

MXenes have been successfully employed as delivery carriers in various forms, including hydrogels, composites,

microneedles, *etc.* Hydrogels are three-dimensional networks of hydrophilic polymers that can absorb and retain large amounts of water or biological fluids, making them excellent candidates for drug delivery systems.<sup>66</sup> MXene-based hydrogels can be designed to provide a suitable microenvironment for wound healing by controlling the release of therapeutic agents, promoting cell proliferation and migration, and improving angiogenesis.<sup>67</sup> Besides, the incorporation of MXenes into hydrogels can enhance their mechanical properties, such as stiffness and toughness, which are essential for the protection and support of the wound site. Numerous studies investigated the use of MXene-based hydrogels for the treatment of chronic wounds.<sup>68–70</sup> As an example, hydrogels were loaded with platelet-derived growth factor (PDGF), a growth factor that promotes cell proliferation and migration. The results of this study confirmed better performance of MXene-based hydrogels in healing wounds compared to control groups, *via* accelerating tissue regeneration and improving wound closure.<sup>71</sup>

As a case study, an intelligent MXene-based hydrogel drug delivery system was fabricated by a research group and consisted of magnetic colloids wrapped with MXene and a dual-network hydrogel composed of poly(*N*-isopropyl acrylamide) and alginate.<sup>72</sup> Exposing to NIR irradiation led to increasing the temperature more than the lower critical solution temperature (LCST) that induced shrinkage of the hydrogel and release of the Ag nanoparticles (NPs) in a controllable manner. The fabricated system demonstrated high reaction capacities and regulated drug delivery capability, allowing it to decrease the harmful side effects of drugs and speed up the healing of wounds. The fabricated hydrogel was applied for the treatment of full-thickness cutaneous wounds and subcutaneously infected wounds in a rat model that confirmed its practical performance.<sup>72</sup> Results showed promising outcomes, indicating the potential application of this system in clinical wound healing and other biomedical fields.

MXene-based hydrogels also have the capability of improving angiogenesis, which is critical for wound healing as it provides oxygen and nutrients to the wound site.<sup>73</sup> Indeed, due to its excellent electrical conductivity, MXene could induce angiogenesis through electrical stimulation. For instance, a high-strength, conductive, and antibacterial polyvinyl alcohol (PVA) hydrogel incorporating  $\text{Ti}_3\text{C}_2\text{T}_x$  (MXene) and polyaniline (PANI) was fabricated by a research group for wound healing applications.<sup>74</sup> The presence of MXene improved the hydrogen bonding between PVA molecules, enhanced the mechanical properties of the hydrogel, and provided antibacterial properties when exposed to NIR light. PANI acted as an electrical conductor and formed chemical bonds with PVA through polymerization, which enhanced the mechanical strength of the hydrogels. The findings of this study indicated that polyvinyl alcohol/MXene/polyaniline (PMP) hydrogels enhanced skin wound healing by stimulating angiogenesis and promoting collagen deposition.<sup>74</sup> MXenes also act as carrier for the delivery of compounds that are responsible for angiogenesis enhancement.<sup>75–77</sup> For instance, the integration of MXene into the structure of microneedle patches had shown promise in enhancing angiogenesis and promoting wound healing *via*



controlling the release of angiogenic factors, which stimulate the growth of new blood vessels and promote tissue regeneration. The employment of MXenes in the structure of micro-needle dressing provides the capability of controlled drug release (*via* NIR irradiation) from one side and real-time monitoring of motion sensing (through its electrical behavior), from the other side.<sup>78</sup>

MXene was integrated with the host material for the micro-needle patches, including 3-(acrylamido)phenylboronic acid (PBA) combined with a polythene glycol diacrylate (PEGDA) hydrogel (Fig. 3).<sup>77</sup> Due to the MXene's ability to retain the stimulation signal at the injury site through photo-thermal conversion, the release of loaded adenosine was accelerated under NIR irradiation. *In vitro* cell experiments confirmed the effectiveness of the adenosine-encapsulated microneedle with MXene integration in improving angiogenesis. The controlled release of adenosine, a therapeutic compound, from this microneedle led to healing the wound *via* fibrosis promotion, matrix production, and angiogenesis.<sup>77</sup>

In recent years, theranostic compounds have been introduced for the simultaneous treatment and real-time monitoring

process that is essential for wound management. In a recent study, a type of smart fabric was fabricated using a thermoresponsive electrospun PHCE film (composed of polycaprolactone, hydroxypropyl cellulose, and ciprofloxacin) that contained an antibiotic, a multilayered MXene-optimized film (MCCF, composed of carbon nanotubes (CNTs), MXene ( $\text{Ti}_3\text{C}_2\text{T}_x$ ), carboxylated cellulose nanofibers (CNFs), thermoplastic polyurethane (TPU) treated with oxygen plasma, silver paste, and poly(dimethylsiloxane) (PDMS)), and the control module (composed of FPCB connected with a temperature sensor and Bluetooth module). Here, the electrospun PHCE film, which was in contact with the wound bed, acted as the extracellular matrix (ECM) from one side, and induced cell migration and proliferation, and induced antibacterial activity, from the other side. The second layer, MCCF, could provide ideal heating performance and durability, and finally the third layer acted as the sensor for real-time monitoring of wound's temperature as well as controlling temperature. Results of this study showed that the fabricated formulation could detect increasing temperature related to wound infection and could therefore be applied for the early detection of infection. On the other hand,

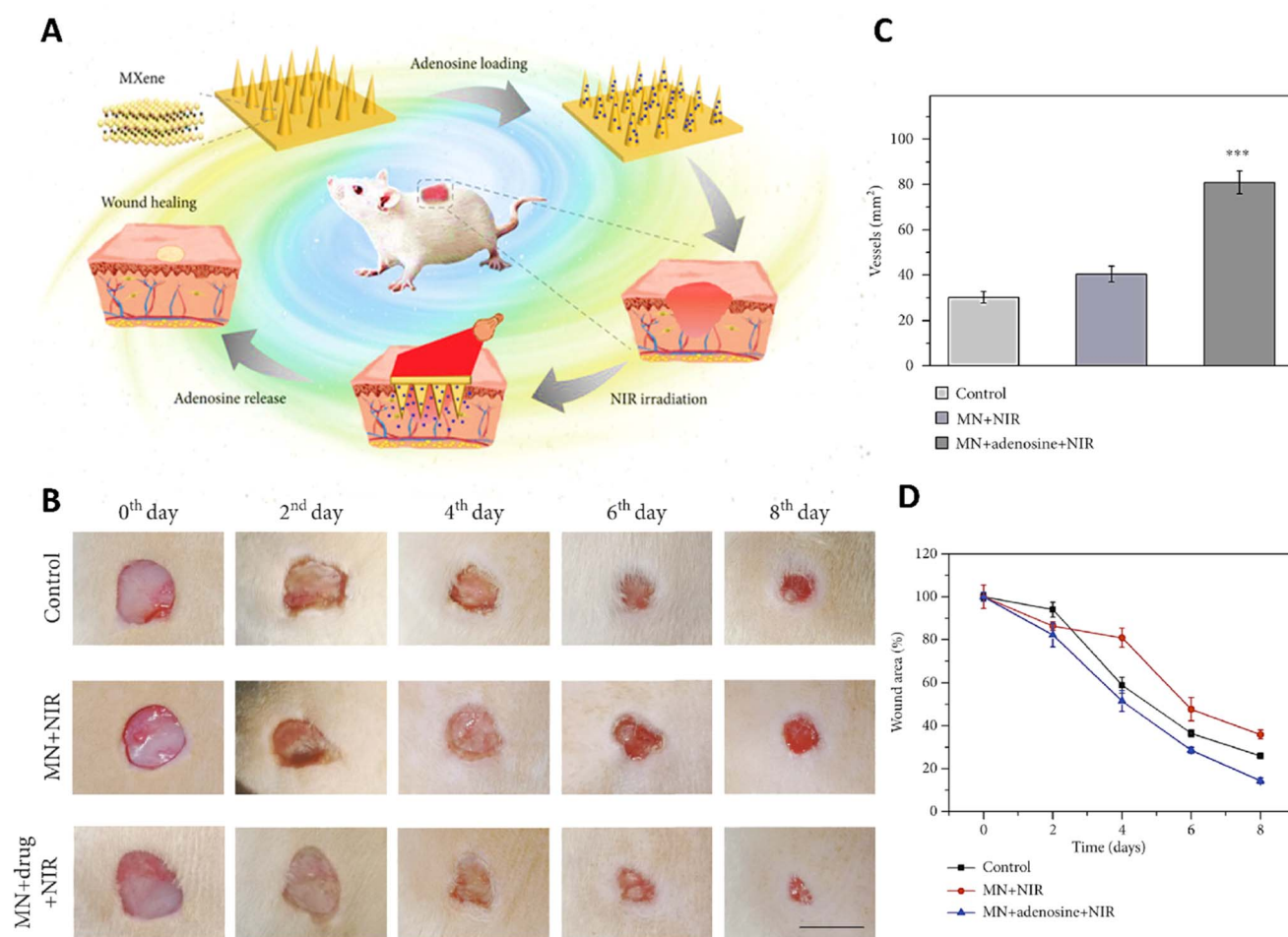
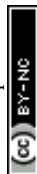


**Fig. 3** Application of MXene based microneedles for wound healing. (A) Schematic illustration of microneedles composed of MXene loaded with adenosine used as a wound healing patch. (B) Healing process of the wound for 8 days after exposure to different treatments. Quantitative results of (C) wound area and (D) vascular structure treated with different formulations. Reprinted with permission from.<sup>77</sup> Distributed under a Creative Commons Attribution License (CC BY 4.0).



the wireless connection between this fabric and a smartphone provided the capability of controlling temperature enhancement by the MCCF layer to near 45 °C, to prevent any side-effects on the skin. Applying a very low voltage led to increasing the temperature and releasing the antibiotic from the system. Results of *in vivo* tests confirmed the effectiveness of this formulation in enhancing the rate of wound healing through inducing the formation of epidermis and dermis and collagen deposition. Increasing the temperature led to the release of therapeutic compounds from the PHCE film in a controllable manner and inducing antibacterial activity.<sup>79</sup>

Overall, MXene-based materials have emerged as promising candidates for drug delivery to wounds due to their unique properties such as high surface areas, excellent biocompatibility, and tunable surface chemistry, enabling efficient loading and controlled release of therapeutic agents. Moreover, they could exhibit inherent antibacterial properties, which can help prevent infections at wound sites, while their biodegradability ensures safe degradation within the body. Their versatility allows for the customization of MXene-based drug delivery systems to meet specific wound healing requirements, making them invaluable tools in the development of advanced wound treatment strategies. However, some specific properties of these materials need to be improved for their commercial application including their safety, which means short-term and long-term toxicity, and their effectiveness in therapy especially when used in combination with traditional strategies.

## 4.2 Tissue regeneration

MXene-based composites can be engineered to possess desired mechanical properties, such as flexibility and elasticity, effectively improving wound healing and providing necessary support for tissue regeneration.<sup>80</sup> One study found that MXene-based composites had a high mechanical strength and could maintain their mechanical properties even after immersing in simulated body fluids for up to seven days.<sup>81</sup> MXenes can be utilized as conductive elements in wound dressings, allowing for the delivery of electrical signals to the wound site. This electrical stimulation can help in regulating cell behavior, promoting tissue regeneration, and accelerating wound closure.<sup>82,83</sup>

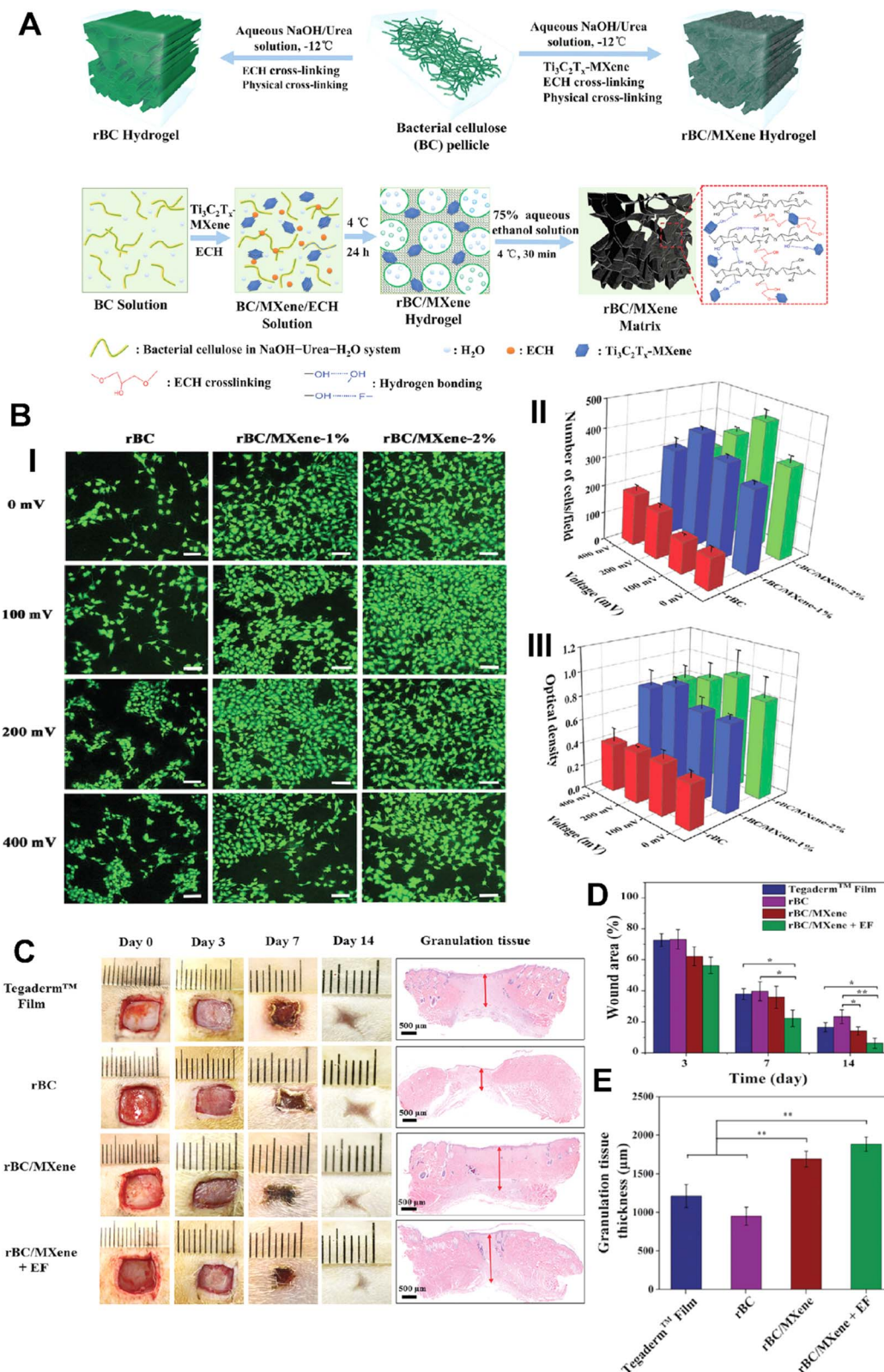
In research conducted by Mao *et al.*,<sup>69</sup> a novel set of multi-purpose hydrogels was developed using regenerative  $\text{Ti}_3\text{C}_2\text{T}_x$  and bacterial cellulose (rBC), which possess the ability to electrically manipulate cell behavior for efficient wound healing with extrinsic electrical stimulation (ES) (Fig. 4). An amalgam hydrogel comprising 2 wt% MXene (rBC/MXene2%) demonstrated optimal electrical conductivity, biocompatibility, mechanical properties, flexibility, and biodegradability. *In vivo* experiments on rats with full-thickness wound injuries revealed that this rBC/MXene hydrogel exhibited superior healing effects in comparison to conventional Tegaderm films. The combination of hydrogel dressings and external electrical stimulation offered a synergistic treatment approach for accelerating wound healing.<sup>69</sup>

MXene ( $\text{Ti}_3\text{C}_2\text{T}_x$ )@polydopamine (MXene@PDA) nanosheets and polyglycerol-ethylene amine (PGE) were mixed in a study to create HPEM scaffolds (H: HCHO; PE: PGE; M: MXene@PDA), which were then treated with oxidized hyaluronic acid (HCHO).<sup>84</sup> These scaffolds had remarkable rheological qualities, self-healing capacities, electrical conductivity, and tissue adhesion features. Furthermore, the HPEM scaffold promoted cell proliferation and increased the production of genes associated with the muscle actin, collagen III, and vascular endothelial growth factor (VEGF), as well as showed strong antibacterial action against *Escherichia coli* (*E. coli*), *Staphylococcus aureus* (*S. aureus*), and multi-drug resistant *S. aureus* (MRSA).<sup>84</sup> Notably, in a full-thickness MRSA-infected wound model, the HPEM scaffolds were found to facilitate early angiogenesis in infected wounds and significantly enhance the healing of MRSA-infected wounds (Fig. 5).<sup>84</sup>

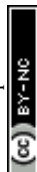
The same researchers prepared composites by combining  $\text{Ti}_3\text{C}_2\text{T}_x$  MXene with antioxidant  $\text{CeO}_2$ .<sup>85</sup> To create FOM scaffolds (F: F127-PEI; O: OSA; M: MXene@ $\text{CeO}_2$ ) within Schiff-based chemically cross-linked hydrogels, MXene@ $\text{CeO}_2$  composites were then added to polyethyleneimine-grafted polythene ions F127 (F127-PEI) and oxidized sodium alginate (OSA). The final FOM scaffolds demonstrated injectability, antimicrobial activity, electrical conductivity, and quick hemostasis, among other useful characteristics. It was demonstrated through *in vitro* and *in vivo* investigations that the FOM scaffolds could facilitate granulated tissue development, collagen deposition, and re-epithelialization as well as enhance fibroblast migration and proliferation. In addition, these scaffolds were able to accelerate the healing of multidrug-resistant (MDR)-infected wounds through electrical stimulation.<sup>85</sup>

Apart from composite scaffold systems derived from diverse materials, researchers have also explored composite hydrogels and sponges for skin dressing applications. A research group conducted a study in which they developed anisotropic MXene@PVA hydrogels using the directional freezing-assisted salting out method.<sup>86</sup> This hydrogel demonstrated excellent mechanical properties, photothermal effects, and broad-spectrum antibacterial activity and promoted cell proliferation. In a mouse wound model, it effectively prevented infection and facilitated skin wound healing with a high closure rate. The MXene@PVA hydrogel exhibited high toughness and anisotropy and could be considered a candidate material for wound dressings with antibacterial, proliferative, and hemostatic properties.<sup>86</sup> To achieve hemostasis and accelerate wound healing, a different team created a composite sponge by fusing MXene-based NPs into a chitin sponge (CH) network. The addition of MXene-based nanomaterials in the structure of sponge significantly enhanced the hemostatic effect of the composite by improving its hemophilicity and accelerating blood coagulation kinetics. In the absence of NIR irradiation, MXene showed about 20–40% reduction in the bacterial colony forming due to its interaction with the bacterial cell wall or membrane and destroying them, while utilizing NIR led to increasing the antibacterial ability to about 100% that could be due to the synergistic effect of MXene capturing and the photothermal effect. It could also facilitate healing of wounds *via*





**Fig. 4** (A) Scheme image of the fabrication process of BC/MXene composite hydrogels. (B) (i) Laser scanning confocal microscopy results of live/dead imaging of NIH3T3 cells treated with different formulations (scale bar = 100  $\mu\text{m}$ ). Number (ii) and viability (iii) of NIH3T3 cells treated with different formulations for 3 days. (C) Photographs of the wounds on days 0, 3, 7, and 14 taken to observe the effect of the dressings on wound healing, with specific focus given to granulation tissue (indicated by red arrows). Quantitative data of wound area as a function of time (D) and granulation tissue thickness on day 14 (E) for each treated group (\* $p < 0.05$  and \*\* $p < 0.01$ ). Reprinted with permission from ref. 69. Copyright 2020, Wiley-VCH GmbH.



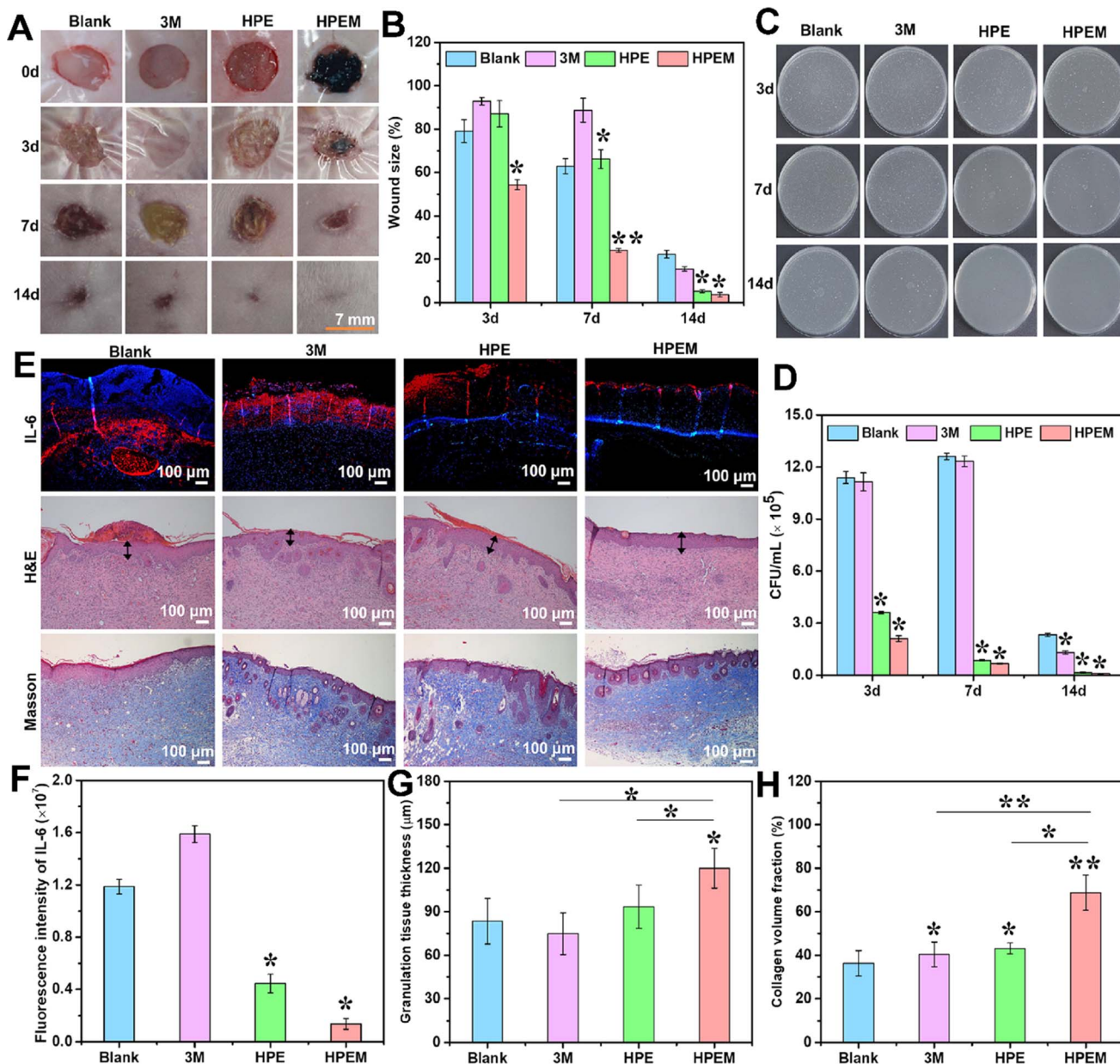


Fig. 5 The results of *in vivo* experiments conducted to assess the anti-infection and wound healing properties of HPEM scaffolds. (A) The skin wound images taken at different time points (0, 3, 7, and 14 days). (B) Comparison between the wound area sizes of different scaffolds (\* $p < 0.05$ , \*\* $p < 0.01$ ). (C) Colony counting assay of MRSA derived from homogenized infected tissues after various treatments on 3, 7, and 14 days. (D) The quantitative bacterial colony densities. (E) IL-6 immunofluorescence images on day 3 and the H&E and Masson's trichrome staining of wound tissues on day 14. The granulation layers in wound beds are indicated with black arrows. Corresponding quantification of (F) fluorescence intensity of IL-6, (G) granulation tissue thickness, and (H) collagen content in wound tissues based on panel E (scale bar = 100  $\mu$ m,  $n = 6$ ; \* $p < 0.05$  and \*\* $p < 0.01$ ). Reprinted with permission from ref. 84. Copyright 2021, American Chemical Society.

enhancing collagen deposition and angiogenesis, so the results of *in vivo* experiments demonstrated about an 84% wound closure rate over 9 days.<sup>87</sup>

In a recent study, a type of electronic skin (E-skin) was fabricated for simultaneous monitoring and healing of diabetic wounds (PPMAG hydrogel). It was composed of MXene sheets covered with polydopamine (PDA) and then doped with Ag NPs, which were then dispersed in a polymeric matrix (P(AM-co-SBMA)) composed of acrylamide (AM) and 2-(methacryloyloxy)-ethyltrimethyl-(3-sulfopropyl) ammonium hydroxide (SBMA).

Here, PDA acted as a mussel inspired compound and improved the adhesiveness, conductivity, and mechanical performance of MXenes and the presence of Ag NPs could induce antibacterial activity. The fabricated formulation showed high antibacterial activity resulting from the presence of Ag NPs, MXene (due to its "nano-knife" ability and ROS capability), and PDA compound (that could affect the bacterial membrane and also denature proteins). It was also shown that the combination of PPMAG hydrogel and electrical stimulation (ES) led to an enhanced healing process for diabetic wounds and skin regeneration.<sup>88</sup>

A type of single-electrode MXene-based wearable triboelectric nanogenerator (TENG) skin patch (TESP) was fabricated *via* using MXene nanosheets entrapped inside a gelatin hydrogel and then this layer was sandwiched by two layers of Ecoflex<sup>®</sup> rubber. Here, gelatin provided different characteristics for the electrolyte (including a low modulus, continuity, and shape adaptability), while MXene enhanced the electrical conductivity and photothermal conversion capabilities of the electrolyte. This patch not only harnesses the combined effects of electrical stimulation and photothermal heating for wound healing but also serves as a motion detector for detecting movements such as finger touches and utilizing the identified electrical pulses to monitor mouse body motions. Here, exposing the patch to NIR laser light led to increasing the temperature to about 45 °C that enhanced the proliferation (76.2% compared to 23.3% in the control group) and migration ability of fibroblast cells. On the other hand, this patch had improved the healing rate of wounds and skin regeneration *via* upregulating the expression of  $\alpha$ -smooth muscle actin ( $\alpha$ -SMA) and vascular endothelial growth factor (VEGF) and enhancing angiogenesis, tissue remodeling, and collagen deposition.<sup>89</sup>

MXenes have shown great potential in biomedical applications, particularly in tissue engineering, due to their unique properties such as ultrathin structure and specific morphologies. They can be easily fabricated and functionalized for various medical uses, including cancer treatment and tissue regeneration. MXene nanocomposites have demonstrated efficiency in targeting malignant cells and antimicrobial properties. Future research is needed to explore their potential in regenerative medicine, sensing applications, and eco-friendly fabrication methods. It is important to evaluate their toxicity, biodegradability, and biocompatibility for safe use in medical applications. Biofunctionalization and chemical modifications can help enhance their stability and targeting properties while reducing adverse effects.

### 4.3 Anti-inflammatory effects

Inflammation is a natural response to tissue injury, which could affect the healing process and prolong this process.<sup>90</sup> MXenes can modulate the inflammatory response by regulating the secretion of inflammatory mediators and promoting a more balanced immune response.<sup>91,92</sup> By reducing excessive inflammation, MXenes facilitate an environment conducive to healing the wound and regenerating damaged tissue.<sup>93,94</sup> Several studies have shown that MXenes, such as titanium carbide ( $\text{Ti}_3\text{C}_2\text{T}_x$ ) and titanium nitride (TiN), can suppress the production of pro-inflammatory mediators, including cytokines and chemokines, which are typically elevated during inflammation.<sup>95,96</sup> By reducing the inflammatory response, MXenes promote a balanced immune response, allowing for more efficient wound healing. One mechanism through which MXenes exert their anti-inflammatory effects is modulation of the activity of immune cells.<sup>97</sup> It is shown that MXenes have the ability to regulate the behavior of macrophages, the key immune cells involved in wound healing and inflammation. They could induce macrophages to shift from the pro-inflammatory (M1)

phenotype to the anti-inflammatory (M2) phenotype, promoting tissue repair and reducing excessive inflammation.<sup>98</sup>

MXenes possess antioxidant properties that can help counteract oxidative stress, a common occurrence during inflammation and wound healing. MXenes can scavenge ROS and protect cells from oxidative damage.<sup>99</sup> By reducing oxidative stress, MXenes contribute to a less inflammatory wound microenvironment and support tissue regeneration. The unique surface chemistry of MXenes also plays a role in their anti-inflammatory effects. Surface functionalization of MXenes can further enhance their anti-inflammatory properties and enable targeted interactions with immune cells.<sup>100</sup> Functional groups, such as carboxyl or amine groups, can be introduced on the MXene surface to enhance their biocompatibility and modulate immune responses. These modifications allow for a more tailored and controlled approach to regulating inflammation and promoting wound healing.<sup>101</sup> However, it is also important to mention that some types of MXenes could produce ROS in direct contact with the cells that could lead to toxicity effects. Thus, it is critical to use surface modification or choose the correct type of MXene for antioxidant applications. For instance, a novel spongy macroporous hydrogel based on poly(acrylamide) (PAAM) was created by a research group, and MXene was added to the hydrogel to provide it with outstanding antibacterial capabilities and an active oxygen scavenging ability.<sup>102</sup> MXene-containing hydrogels showed a reactive oxygen scavenging rate of up to 96%. Scientists hypothesized that this was primarily caused by the antioxidant phenol quinone groups in the polymer chain removing ROS by a redox reaction, which was further improved by the electron transport capability of MXene.<sup>102</sup>

A temperature-sensitive  $\text{Nb}_2\text{C}$  hydrogel composed of  $\text{Nb}_2\text{C}$  and poly (lactic-co-glycolic acid) (PLGA)-polythene glycol (PEG)-PLGA triblock copolymer with antioxidant and antibacterial properties was created by another research group.<sup>103</sup> This hydrogel could efficiently eliminate ROS and reduce oxidative cell damage due to the presence of  $\text{Nb}_2\text{C}$  nanosheets. In addition, the hydrogel exposed to NIR radiation possesses high antibacterial activity against both Gram-positive and Gram-negative bacterial strains due to the photothermal ability of MXene nanosheets. This ROS scavenging ability of this formulation led to acceleration of the healing process through enhancing re-epithelialization and angiogenesis and deposition of collagen.

Li *et al.* developed an injectable hydrogel for diabetic wound healing that was composed of hyaluronic acid-*graft*-dopamine and polydopamine coated  $\text{Ti}_3\text{C}_2$  MXene nanosheets (Fig. 6).<sup>104</sup> MXene in the hydrogel could scavenge excessive reactive nitrogen species and ROS to alleviate oxidative stress and eradicate bacteria. The hydrogel also regulates macrophage polarization from M1 to M2 resulting in anti-inflammatory effects. When combined with mild photothermal stimulation, it significantly enhanced human umbilical vein endothelial cell proliferation and migration and effectively facilitated the healing of infected diabetic wounds.<sup>104</sup>

This injectable hydrogel used dopamine-grafted hyaluronic acid (HA-DA) and polydopamine (PDA)-coated  $\text{Ti}_3\text{C}_2$  MXene



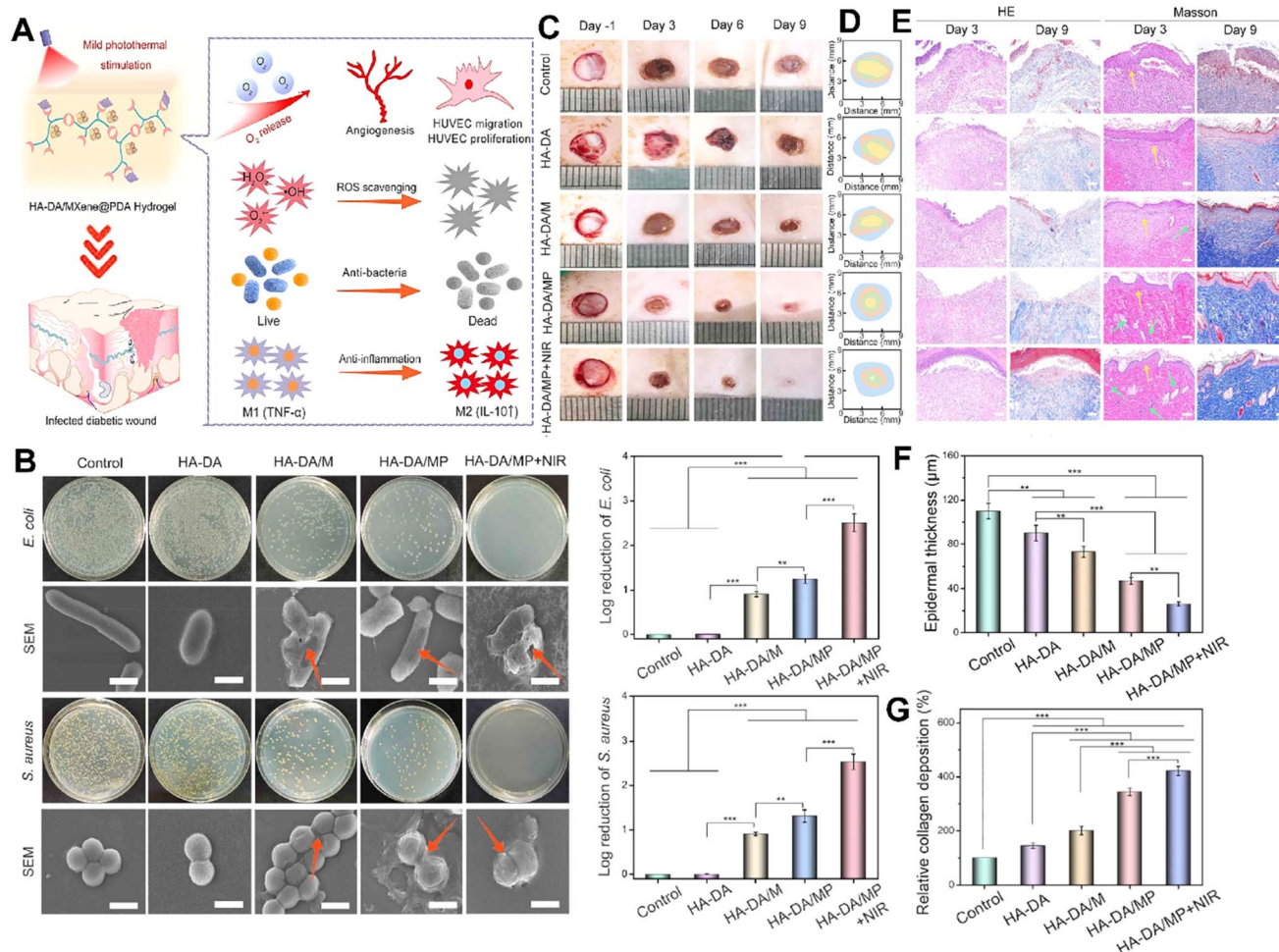


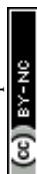
**Fig. 6** (A) Schematic illustration showing the treatment mechanisms used by the HA-DA/MXene@PDA hydrogel for wound healing. (B) Anti-bacterial activity of different formulations after exposure to *E. coli* and *S. aureus*, along with the SEM image and log reduction of bacteria. Photograph (C) and trace (D) of wound closure and histopathological image (E) of the wound treated with different formulations on 1, 3, 6, and 9 days (scale bar = 50  $\mu$ m). Quantitative results of epidermal thickness (F) and collagen deposition (G) after 9 days of treatment (\*\*\* $p$  < 0.001, \*\* $p$  < 0.01, \* $p$  < 0.05). Reprinted with permission from ref. 104. Copyright 2022, American Chemical Society.

nanosheets ( $Ti_3C_2$ @PDA or MXene@PDA NSs) by combining catechol groups with the help of the  $H_2O_2$ /HbO<sub>2</sub> system. By adding dopamine to the HA molecules, the hydrogels gained strong tissue adhesion, preventing bacterial invasion, maintaining moisture, and promoting clotting. In addition, the dopamine molecules in HA-DA-based hydrogels could reduce inflammation by regulating macrophage activity, aiding skin recovery. These injectable hydrogels were proposed for filling wounds' irregular cavities and coming into close contact with wound surfaces to prevent bacterial invasion and maintain moisture, thus decreasing inflammation and promoting diabetic wound healing.<sup>104</sup>

In a recent study, MXene@TiO<sub>2</sub> (MT) nanosheets were dispersed in the structure of a hydrogel composed of gelatin (GA) and oxidized konjac glucomannan (OKGM) (GA/OKGM/MT hydrogel). The fabricated formulation showed good skin adhesiveness, that provided fast hemostasis, strong antibacterial activity, and anti-inflammatory effect, *via* exhibiting antibacterial activity, due to the photothermal ability of MXene@TiO<sub>2</sub> and

reducing the amounts of ROS that induced the healing process from the inflammatory phase to the proliferation phase. The combination use of electrical stimulation (ES) and the fabricated hydrogel accelerated the regeneration of skin wounds *via* inducing migration and proliferation of fibroblast cells, enhancing collagen deposition, and neovascularization.<sup>105</sup>

According to the above-mentioned features, MXenes exhibit significant potential in mitigating inflammation through various mechanisms. For instance, they could scavenge ROS and inhibit inflammatory mediators such as cytokines and chemokines which underscores their anti-inflammatory efficacy. Moreover, high biocompatibility and facile synthesis of MXene make it a compelling candidate for biomedical applications that want to overcome inflammatory conditions. Maintaining a balance between anti-inflammatory effects and promoting suitable vascularization is a key challenge in this field, and MXenes offer a promising solution by providing controlled release of positive factors, creating a suitable thermal environment and having an ideal structure and composition.



#### 4.4 Photothermal effects

The photothermal effect is another important aspect of MXenes that holds significant potential for advanced wound dressing and healing applications.<sup>36</sup> MXenes, such as titanium carbide ( $\text{Ti}_3\text{C}_2$ ), exhibit strong absorption in the NIR region, which allows them to convert light energy into localized heat.<sup>106</sup> This photothermal effect can be harnessed to enhance wound healing through various mechanisms. One of the key advantages of MXene-based photothermal therapy is its ability to selectively target and eliminate bacteria,<sup>107</sup> which is a common challenge in wound care. When exposed to NIR light, MXene could generate localized heat that could effectively kill bacteria by damaging their membranes or denaturing essential proteins, without harming the surrounding healthy tissues.<sup>108</sup> In a study, 0.5 W NIR irradiated for 5 min raised the temperature of the produced nanofiber hydrogel loaded with MXene from 23 °C to 41 °C and 1 W NIR irradiated for 5 min raised the temperature even to 61 °C.<sup>109</sup> This targeted approach offers a promising alternative for combating bacterial infections and reducing the need for systemic antibiotics.<sup>110</sup> To create a multifunctional membrane, researchers created a chitosan-MXene solution and placed it onto a poly(vinylidene fluoride) (PVDF) membrane.<sup>111</sup> The antibacterial experiment findings demonstrated that the multifunctional membrane paired with NIR had a nearly 100% antibacterial ability, which was much better than that of the simple material group without NIR irradiation. According to the findings of animal studies, the NIR irradiation of the formulation showed a healing rate of 95% over 14 days of treatment, which was greater than that by the material group without NIR irradiation. These findings suggested that photothermal action of MXene could enhance its antibacterial characteristics and improve its ability to cure infected wounds.<sup>111</sup>

The photothermal effect of MXenes can also facilitate wound healing by promoting tissue regeneration. Controlled application of localized heat to the wound site can stimulate various cellular processes involved in tissue repair.<sup>112</sup> The heat generated by MXenes under NIR light can increase blood circulation, which helps deliver oxygen and nutrients to the wound area and remove waste products. Enhanced blood flow promotes the migration and proliferation of cells involved in wound healing, such as fibroblasts and endothelial cells.<sup>113</sup> In addition, the heat can induce collagen remodeling and the synthesis of extracellular matrix components, promoting wound closure and tissue regeneration.

A research group introduced a novel approach to produce  $\text{Ti}_3\text{C}_2$  MXene/COL(collagen)/SF(silk fibroin)/quercetin scaffolds (M-CSQ scaffolds) using cryogenic 3D printing and freeze-drying techniques. The M-CSQ scaffold effectively killed oral squamous cell carcinoma (OSCC) cells due to the excellent photothermal conversion properties of  $\text{Ti}_3\text{C}_2$  MXene, while also promoting oral mucosa regeneration (Fig. 7).<sup>113</sup> The presence of quercetin led to the enhancement of thermal sensitivity of the OSCC cells during photothermal therapy (PTT) *via* regulating the expression of heat shock protein 70 (HSP70). The scaffold was gradually degraded over time and facilitated the growth of new oral mucosal tissue with the aid of silk proteins and COL.

Ultimately, through combining 2D  $\text{Ti}_3\text{C}_2$  MXene, quercetin, and the 3D printed tissue engineering scaffold, simultaneous killing of OSCC cells and repair of oral mucosal wounds were successfully attained. Both *in vivo* and *in vitro* experiments demonstrated that the M-CSQ composite scaffold was effective in killing SCC25 and CAL27 cells as well as inhibiting tumor growth.<sup>113</sup>

The photothermal effect of MXenes can also aid in the controlled release of therapeutic agents. By incorporating MXenes into wound dressings or coatings and then applying NIR light, the localized heat can trigger the release of encapsulated bioactive molecules, such as growth factors or antimicrobial agents.<sup>114</sup> This on-demand release mechanism allows for precise temporal and spatial control over the delivery of therapeutic agents, ensuring their effectiveness at the wound site. MXene surfaces can also be modified with specific functional groups or molecules to introduce additional functionalities, such as improved biocompatibility, targeted drug delivery, or enhanced cellular interactions.<sup>115</sup> For instance, a research team created a multi-stimulus response MXene@AgNPs hydrogel that achieved precise, controlled release of AgNPs by the photoreponse and magnetic response, avoided the cytotoxicity that resulted from the release of high concentrations of AgNPs in a brief period of time, and ensured the bactericidal effect.<sup>72</sup> According to the outcomes of animal studies, following the NIR irradiation, the local temperature increased that further elevated depth action of AgNPs and improved the therapeutic impact of the fabricated compound on deep parts of the skin.

A temperature-responsive material was developed using a composite nanobelt polyacrylonitrile and polyvinylpyrrolidone modified with MXene, covered with a layer of thermosensitive copolymers of acrylamide (AAM), acrylonitrile (AN), and vinylimidazole (AAM-*co*-AN-*co*-VIm) (known as PAAV) and used for the delivery of vitamin E.<sup>109</sup> In the presence of NIR irradiation, the photothermal ability of the fabricated formulation was activated that led to increasing the temperature to about 39 °C after just 3 min, in a repeatable way, which was rapidly decreased after removing NIR. This photothermal effect led to activation of thermal responsibility of the PAAV which led to the release of vitamin E in a controllable manner. Exposing the fabricated formulation to real wounds on mice confirmed its effectiveness in healing wounds *via* inducing angiogenesis and promoting cell proliferation (due to the presence of both vitamin E and the photothermal effect).<sup>109</sup>

A new antibacterial platform was introduced by a team, which is based on the Schottky junction of bioactive zinc-based metal-organic framework (Zn-MOF) and  $\text{Ti}_3\text{C}_2\text{T}_x$  nanosheets (known as Zn-MOF@ $\text{Ti}_3\text{C}_2\text{T}_x$ ). Zn-MOF has a porous accordion-like structure, high porosity, and rich Zn 2p content. On the other hand,  $\text{Ti}_3\text{C}_2\text{T}_x$  nanosheets show excellent photothermal performance with a high conversion rate. The resulting Zn-MOF@ $\text{Ti}_3\text{C}_2\text{T}_x$  hybrid can release  $\text{Zn}^{2+}$  and curcumin in a controlled and accelerated manner under NIR irradiation.<sup>116</sup>

Accordingly, the photothermal ability of MXenes is a promising way of enhancing wound healing through employing different mechanisms. They could be used for enhancing various processes such as cell proliferation, angiogenesis, and



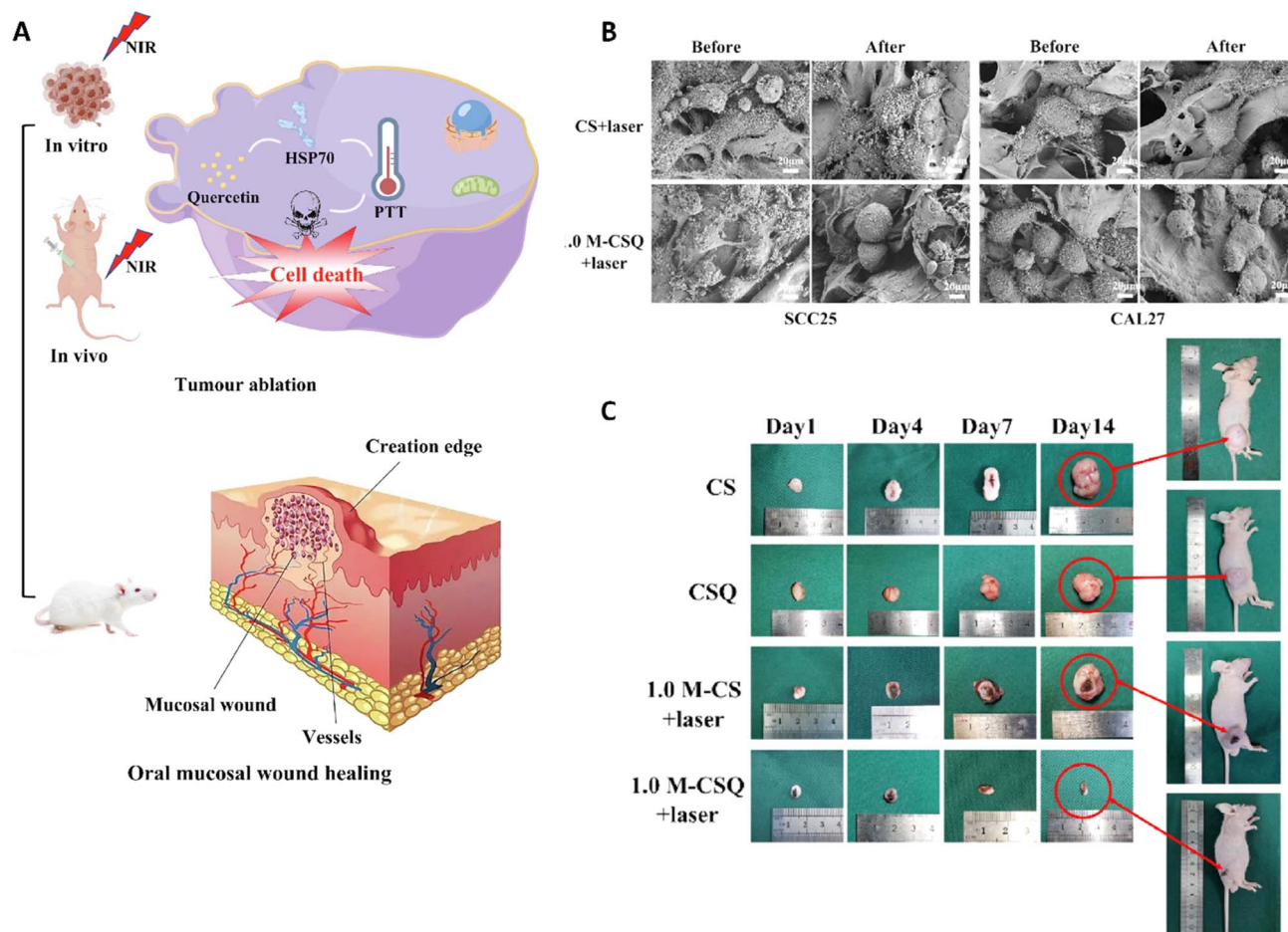


Fig. 7 (A) Application of the M-CSQ scaffold for the treatment and reconstruction of oral mucosal wounds. (B) Scanning electron microscopy (SEM) image of SCC25 and CAL27 cells before and after exposure to two different formulations. (C) The photograph of tumor size after treating with different scaffolds on 1, 4, 7, and 14 days. Reprinted with permission from ref. 113. Copyright 2023, Elsevier.

extracellular matrix deposition or could facilitate the controlled release of therapeutic agents and so enhance their potential for accelerating wound closure and tissue regeneration. This photothermal effect could also be used for killing bacteria, thus providing the antibacterial activity of the wound dressing material on one side and preventing the bacterial drug resistance on the other side.

#### 4.5 Hemostatic facility

MXenes could also promote hemostasis making them promising candidates for applications in wound management and control of bleeding.<sup>117</sup> One key factor contributing to the hemostatic ability of MXenes is their highly porous structure, which allows for efficient absorption and entrapment of blood components. MXenes possess a large specific surface area and interconnected pore networks that facilitate the rapid adhesion and aggregation of blood cells, platelets, and fibrinogen.<sup>118,119</sup> On the other hand, MXene contains a strong surface charge that encourages platelet activation, blood cell aggregation, and clot formation.<sup>120</sup> This aggregation process aids in the formation of a stable clot and the promotion of coagulation, thereby effectively controlling bleeding.<sup>121</sup> The surface chemistry of MXenes

can be tailored to enhance their interaction with blood components and promote coagulation.<sup>122</sup> Surface modifications, such as functionalization with carboxyl or amine groups, have been shown to improve the adhesion of platelets and the activation of clotting factors, further enhancing hemostatic properties. One such example is an MXene@polydopamine (PDA) decorated chitosan nanofiber wound treatment mat, which showed better blood cell and platelet adhesion in both *in vitro* and *in vivo* studies.<sup>123</sup> This was mostly due to the high concentration of hydroxyl groups in MXene@PDA, which could adhere to the blood cells and platelets and, upon coming into contact with plasma fibrin, trigger blood cell aggregation, platelet activation, and clot formation. Another team created an antibacterial fiber membrane made of electrospun poly(polycaprolactone) scaffolds and polydopamine-coated MXene/Ag<sub>3</sub>PO<sub>4</sub> bioheterojunctions (MX@AgP bio-HJs) in order to employ NIR to accomplish sterilization and hemostasis and to encourage the growth of new collagen and epithelial tissue. Exposing the fabricated scaffold to NIR illumination led to release of Ag<sup>+</sup> ions from MX@AgP NPs in the membrane that resulted in an excellent bactericidal effect. Polydopamine reduces Ag<sup>+</sup> ions back to Ag<sup>0</sup> NPs, enabling the self-

rechargeability of  $\text{Ag}^+$  ions for subsequent phototherapy. *In vivo* experiments, on the other hand, demonstrated that the photo-activated nanofibrous membranes created a regenerative wound microenvironment by eliminating bacteria, stopping bleeding, and promoting epithelialization, collagen deposition, and angiogenesis (Fig. 8).<sup>124</sup>

Overall, MXenes demonstrate remarkable hemostatic properties, characterized by their ability to rapidly induce blood clot formation upon contact with blood, which is related to their high surface area and surface chemistry, which promote platelet adhesion and activation, leading to efficient hemostasis. By quickly stopping bleeding, MXenes not only minimize blood loss but also create an optimal environment for subsequent wound healing processes. The prompt initiation of clotting helps establish a scaffold for tissue repair and reduces the risk of infection, ultimately promoting faster and more effective wound closure.

In Table 1, some of the other samples related to the application of MXene based materials for wound healing applications are summarized.

## 5. Challenges

### 5.1 MXene production

One of the primary challenges of MXene-based composites is the difficulty of producing large-scale materials with homogeneous features. MXenes are typically synthesized by etching MAX phases, which involves the use of hydrofluoric acid, a highly corrosive and toxic substance. The synthesis of MXenes

also requires precise control over the reaction conditions, which can be challenging to achieve at scale. Furthermore, the synthesis of MXenes is a time-consuming process, and the yield of the product can be low. Besides, dose, size, and surface modifications of MXenes could affect their biocompatibility. They also need surface modification to avoid loss of their functional and structural properties and prevent their oxidation.<sup>60,133</sup> To overcome these challenges, researchers have developed several approaches for large-scale production of MXenes. One approach involves the use of safer and more environmentally friendly etchants, such as sodium hydroxide or ammonium fluoride, instead of hydrofluoric acid. Another approach involves the use of advanced processing techniques, such as microwave irradiation, to enhance the yield and reduce the synthesis time of MXenes. Researchers have also explored the use of continuous flow reactors and other process intensification techniques to improve the scalability of MXene synthesis.<sup>134,135</sup>

### 5.2 Economic challenges

Another challenge of MXene-based composites is the cost of production and economic viability. The synthesis of MXenes involves the use of expensive precursor materials, such as titanium and aluminum, and the use of advanced processing techniques, which can increase the production cost. Furthermore, the use of MXenes in wound healing and dressings requires the development of specialized manufacturing processes, which can further increase the production cost. To overcome these challenges, researchers have explored several

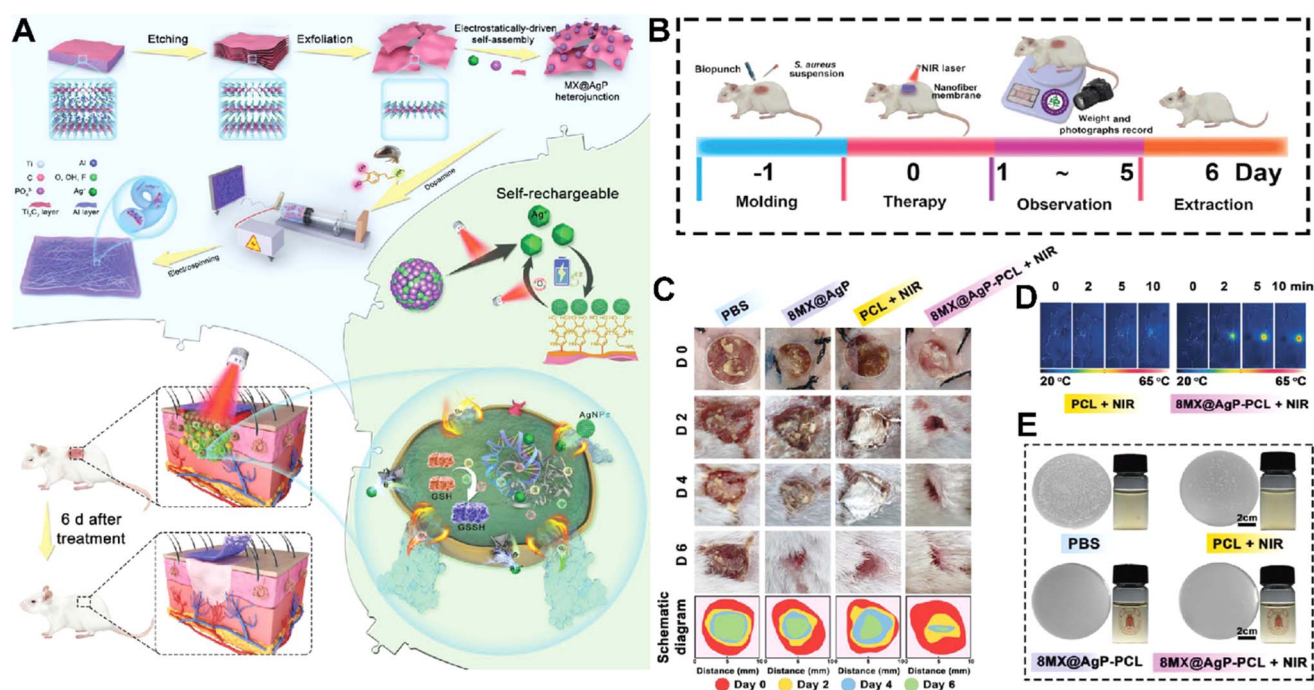


Fig. 8 (A) Schematic illustration of fabrication and application of the MX@AgP-PCL membranes. The *in vivo* experimental process (B) and wound healing procedure (C) after treating with different formulations. (D) NIR image of the membrane after different times of exposure to NIR light. (E) Colony counting results of different formulations exposed to *S. aureus*. Reprinted with permission from ref. 124. Copyright 2022, Wiley-VCH GmbH.



Table 1 The application of MXene-based composites in wound healing

Formulation	MXene effect	Main achievements	Ref.
Chitin/MXene composite sponges (CH/Au@sMX sponges)	Improving the hemostatic efficacy <i>via</i> enhancing the haemocompatibility and increasing the coagulation rate and enhancing the antibacterial activity through the NIR effect	Accelerating wound healing <i>via</i> exhibiting predominant antibacterial activity, enhanced hemostatic performance and promoting normal cell migration	87
MXene/PVA hydrogel	Improving the antibacterial activity <i>via</i> the hyperthermia effect	Fabricating hydrogels with ideal mechanical properties and broad-spectrum antibacterial activity, promoting cell proliferation and inhibiting wound infection	86
MXene-loaded nanofibers (MNFs) covered with dopamine-hyaluronic acid hydrogel (H) loaded vascular endothelial growth factor, (V), (MNFs@V-H@DA) hybrid hydrogels	Regulating neovascularization <i>via</i> controlled release of growth factor and helping in achieving scarless healing <i>via</i> NIR-photoresponsivity	Improving the healing of wounds and skin regeneration <i>via</i> modulating the immune microenvironment, inhibiting inflammatory effects, inhibiting excessive neovascularization and extracellular matrix deposition	125
Polyvinyl alcohol/MXene/polyaniline hydrogels	Improving the mechanical properties of the hydrogel and providing antibacterial activity <i>via</i> the NIR effect	Fabricating hydrogels with good mechanical properties, electrical conductivity, antibacterial activity, capability of promoting cell proliferation and migration, and ability to accelerate skin wound healing through improving angiogenesis and collagen deposition	74
Amoxicillin (AMX), MXene, and polyvinyl alcohol (PVA) (MXene-AMX-PVA) nanofibrous membrane	Providing controlled drug release <i>via</i> local hyperthermia	Bacteriostatic activity and wound healing capability	11
Titanium carbide (MXene)/zeolite imidazole framework-8 (ZIF-8)/polylactic acid (PLA) composite membrane (MZ-8/PLA)	Antibacterial activity that resulted from NIR irradiation	Fabricating a smart responsive platform with: anticancer activity <i>via</i> photothermal and photodynamic therapy, antibacterial activity, and wound healing capability	126
Bi <sub>2</sub> S <sub>3</sub> /Ti <sub>3</sub> C <sub>2</sub> T <sub>x</sub> MXene interfacial Schottky junction	Antibacterial activity	Eliminating bacterial infection <i>via</i> producing an ecofriendly photoresponsive Schottky junction platform	127
Electrospun poly (lactic-co-glycolic acid) (PLGA) scaffolds, MXene/Ag <sub>2</sub> S	Sterilizing the wound <i>via</i> producing H <sub>2</sub> O <sub>2</sub> and antibacterial activity resulting from producing reactive oxygen species <i>via</i> NIR	Promoting wound regeneration <i>via</i> improving the local deposition of collagen, promoting angiogenesis, antibacterial activity, and stopping bleeding,	128
Nano-platform-scaffold of Ti <sub>3</sub> C <sub>2</sub> MXene/MoS <sub>2</sub> (MM)	Antibacterial activity resulting from NIR irradiation	Providing antibacterial activity resulting from four different mechanisms: photothermal and photodynamic activity along with peroxidase-like (POD-like) and glutathione oxidase-like properties and improving tissue regeneration <i>via</i> promoting skin cell migration	129
K-M/PNIPAm hydrogel	NIR-controlled drug release	Fabrication of an intelligent hydrogel with the capability of real-time monitoring of health and NIR responsive controlled drug release	130
MXene and spidroin-incorporated microneedle scaffolds	Providing the capability of sensitive monitoring of wound movement and controlled drug release using NIR irradiation	Fabrication of microneedles with high self-healing and mechanical performance and promoting wound healing <i>via</i> light responsive release of drug	131



Table 1 (Contd.)

Formulation	MXene effect	Main achievements	Ref.
Electrospun $\text{Ti}_3\text{C}_2\text{T}_x$ /chitosan nanofibers	Antibacterial activity	Producing a low-cost, high biocompatible and biodegradable wound dressing mat with good antibacterial activity	12
NIR-responsive MXene nanofibers and hydrogel double structure system (MNFs@DFOM-H@AC)	Controlling angiogenesis and the immune microenvironment <i>via</i> controlled release of drugs	Fabrication of a wound dressing hydrogel with anti-inflammatory capability, appropriate vascularization, and controlled release of therapeutic compounds	132
Lens epithelial cells by $\text{Ti}_3\text{C}_2\text{T}_x$ MXene coatings	Reducing the expression of cytokines, preventing the epithelial-mesenchymal transition, downregulating mechanisms related to myofibroblast transdifferentiation and migration, and promoting wound healing	Developing intraocular lens devices with the ability to suppress hyperinflammation, prevent the epithelial-mesenchymal transition, and reduce posterior capsule opacification	8

approaches to reduce the cost of production of MXene-based composites. One approach involves the use of alternative precursor materials, such as iron or manganese, which are less expensive than titanium and aluminum. Another approach involves the development of simpler and more cost-effective processing techniques, such as ball milling or ultrasonication, for the synthesis of MXenes. Researchers have also explored the use of low-cost and scalable manufacturing processes, such as electrospinning or 3D printing, for the production of MXene-based wound dressings.<sup>136,137</sup>

### 5.3 Stability

The stability of MXene-based composites is another challenge that needs to be addressed. MXenes are susceptible to oxidation and degradation, particularly when exposed to air or moisture. The stability of MXene-based composites can be further compromised when exposed to biological fluids, such as blood or wound exudate, which can contain enzymes and other reactive species that can degrade the material. To improve the stability of MXene-based composites, researchers have explored several approaches. One approach involves the use of protective coatings, such as graphene or polymer coatings, to prevent oxidation and degradation of the MXene nanosheets. Another approach involves the use of crosslinking agents, such as glutaraldehyde or genipin, to enhance the stability of MXene-based composites. Researchers have also explored the use of hybrid materials, such as MXene-silk or MXene-collagen composites, to improve the stability and biocompatibility of MXene-based composites.<sup>138,139</sup>

### 5.4 Environmental effect

The environmental impact of MXene-based composites is another issue that needs to be considered. The synthesis of MXenes involves the use of chemicals and energy, which can have a significant environmental impact. Furthermore, the disposal of MXene-based composites at the end of their useful

life can also have an environmental impact, particularly if the materials are not biodegradable or recyclable. To address the environmental impact of MXene-based composites, researchers have explored several approaches. One approach involves the use of green chemistry principles in the synthesis of MXenes, such as the use of safer etchants and solvents and the use of renewable energy sources. Another approach involves the development of biodegradable and recyclable MXene-based composites, such as MXene-cellulose composites or MXene-chitosan composites. Researchers have also explored the use of waste materials, such as agricultural waste or industrial by-products, as precursors for MXene synthesis, to reduce the environmental impact of the materials.<sup>140–142</sup>

### 5.5 Long-term biocompatibility issues

The biosafety and regulatory issues regarding the clinical applications of MXene-based composites are also important to consider. MXenes are relatively new materials, and their long-term safety and biocompatibility are not fully understood. Furthermore, the use of MXene-based composites in clinical applications requires regulatory approval, which can be a time-consuming and costly process. To address the biosafety and regulatory issues of MXene-based composites, researchers have conducted extensive biocompatibility studies. These studies have shown that MXene-based composites exhibit low cytotoxicity and are generally well-tolerated by cells and tissues. However, further studies are needed to understand the long-term effects of MXene-based composites on the body. Regarding regulatory issues, researchers and manufacturers of MXene-based composites need to comply with the regulatory requirements of the countries where the materials are intended to be used. The regulatory approval process for medical devices and materials can be complex and can vary between countries. Therefore, it is important for researchers and manufacturers to have a clear understanding of the regulatory requirements before developing and marketing MXene-based composites for clinical applications.<sup>143–145</sup>



## 6. Perspectives

MXene-based composites have also demonstrated the ability to promote tissue regeneration. The incorporation of MXenes into scaffolds or hydrogels can enhance their mechanical properties and improve their biocompatibility. Moreover, MXene-based composites can promote cell proliferation and differentiation, which can accelerate the regeneration of damaged tissues, such as skin. Researchers can further explore the use of MXene-based composites for tissue engineering and regenerative medicine applications, including the development of 3D printed implants, wound dressings, or patches for skin regeneration. The biocompatibility of MXene-based composites is critical for their use in wound healing applications, as they must be able to integrate seamlessly with the surrounding tissue. MXenes have already demonstrated excellent biocompatibility in several *in vitro* and *in vivo* studies, and the incorporation of MXenes into biomaterials can improve their biocompatibility. Researchers can further explore various approaches to improve the biocompatibility of MXene-based composites, such as the use of biodegradable polymers or natural biomolecules, such as collagen or hyaluronic acid. MXene-based composites can also be used for targeted drug delivery, which can improve the therapeutic efficacy of wound healing agents. Researchers have already shown that MXene-based composites can act as carriers for various drugs, such as growth factors, antibiotics, or anti-inflammatory agents. Moreover, the surface of MXenes can be functionalized to target specific cells or tissues, which can enhance the specificity and selectivity of drug delivery. In the future, researchers can explore various approaches to improve the targeted drug delivery of MXene-based composites, such as the use of stimuli-responsive polymers or the incorporation of magnetic NPs.<sup>146–148</sup>

To enable the clinical translation of MXene-based composites in wound healing applications, clinical trials are needed to demonstrate their safety and efficacy in humans. Several preclinical studies have already demonstrated the potential of MXene-based composites in wound healing applications, and the results are promising. However, further studies are needed to evaluate the long-term safety and efficacy of these materials in humans. Moreover, the successful translation of MXene-based composites to the clinic requires collaboration between researchers, manufacturers, clinicians, and regulatory authorities. The development and marketing of MXene-based composites also require regulatory approval from relevant authorities, such as the US Food and Drug Administration (FDA) or the European Medicines Agency (EMA). Researchers must ensure that the materials meet all safety and efficacy standards and comply with all regulatory requirements before clinical trials can be initiated.<sup>149–152</sup>

## 7. Conclusion

MXene-based materials have shown great potential for wound healing/dressing and bactericidal applications owing to their unique properties and biocompatibility. Several studies have investigated the application of MXenes and their composites for

skin wound repair as well as promoting fibroblast migration, showing good biocompatibility and strong bactericidal potential. MXenes possess several properties that make them effective in wound healing, including bactericidal properties, photo-thermal effects, suitable cytocompatibility, rich functional groups, and scavenging ability of active oxygen species. Currently, there exists limited information available on the cost and availability of MXenes compared to traditional wound dressing materials. While traditional wound dressings made of gauze, cotton, and other materials are widely available and cost-effective, the employment of MXenes and their modified composites in wound dressings is still in the early stages of development. Overall, there are limited studies that directly compare the effectiveness of MXene-based composites to traditional wound dressing. However, given the promising results of these materials in wound healing/dressing, it is possible that they may become more widely available and cost-effective in the future. In this context, challenges related to cytotoxicity, long-term biosafety, lack of standardization, cost of production, and environmental impact of production/disposal are among the crucial aspects for future explorations.

## Conflicts of interest

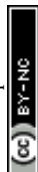
The authors declare no conflict of interest.

## References

- 1 Y. Liang, J. He and B. Guo, *ACS Nano*, 2021, **15**, 12687–12722.
- 2 A. Maleki, J. He, S. Bochari, V. Nosrati, M.-A. Shahbazi and B. Guo, *ACS Nano*, 2021, **15**, 18895–18930.
- 3 D. Khorsandi, J.-W. Yang, Z. Ülker, K. Bayraktaroğlu, A. Zarepour, S. Iravani and A. Khosravi, *Microchem. J.*, 2024, **197**, 109874.
- 4 A. Zarepour, S. Ahmadi, N. Rabiee, A. Zarrabi and S. Iravani, *Nano-Micro Lett.*, 2023, **15**, 100.
- 5 Y. Gogotsi and B. Anasori, *ACS Nano*, 2019, **13**, 8491–8494.
- 6 K. R. G. Lim, M. Shekhirev, B. C. Wyatt, B. Anasori, Y. Gogotsi and Z. W. Seh, *Nat., Synth.*, 2022, **1**, 601–614.
- 7 F. Alimohammadi, M. Sharifian Gh, N. H. Attanayake, A. C. Thenuwara, Y. Gogotsi, B. Anasori and D. R. Strongin, *Langmuir*, 2018, **34**, 7192–7200.
- 8 G. Cooksley, M. K. Dymond, N. A. Stewart, G. Bucca, A. Hesketh, J. Lacey, Y. Gogotsi and S. Sandeman, *2D Mater.*, 2022, **10**, 014003.
- 9 K. Rasool, K. A. Mahmoud, D. J. Johnson, M. Helal, G. R. Berdiyrov and Y. Gogotsi, *Sci. Rep.*, 2017, **7**, 1–11.
- 10 K. Diedkova, A. D. Pogrebnjak, S. Kyrylenko, K. Smyrnova, V. V. Buranich, P. Horodek, P. Zukowski, T. N. Koltunowicz, P. Galaszkiwicz and K. Makashina, *ACS Appl. Mater. Interfaces*, 2023, **15**, 14033–14047.
- 11 X. Xu, S. Wang, H. Wu, Y. Liu, F. Xu and J. Zhao, *Colloids Surf., B*, 2021, **207**, 111979.
- 12 E. A. Mayerberger, R. M. Street, R. M. McDaniel, M. W. Barsoum and C. L. Schauer, *RSC Adv.*, 2018, **8**, 35386–35394.



- 13 H. Zhu, W. Dai, L. Wang, C. Yao, C. Wang, B. Gu, D. Li and J. He, *Polymers*, 2022, **14**, 3908.
- 14 Y. Zhong, S. Huang, Z. Feng, Y. Fu and A. Mo, *J. Biomed. Mater. Res., Part A*, 2022, **110**, 1840–1859.
- 15 H. Park, S. Kim, S. Kim, M. Kim, Y. Kang, S. Amirthalingam, S. Lee, N. S. Hwang, K. Yang and H. D. Kim, *J. Ind. Eng. Chem.*, 2022, **117**, 38–53.
- 16 S. Xu, C. Du, M. Zhang, R. Wang, W. Feng, C. Wang, Q. Liu and W. Zhao, *Nano Res.*, 2023, **16**, 9672–9687.
- 17 H. Riazi, M. Anayee, K. Hantanasirisakul, A. A. Shamsabadi, B. Anasori, Y. Gogotsi and M. Soroush, *Adv. Mater. Interfaces*, 2020, **7**, 1902008.
- 18 L. Chen, F. Chen, G. Liu, H. Lin, Y. Bao, D. Han, W. Wang, Y. Ma, B. Zhang and L. Niu, *Anal. Chem.*, 2022, **94**, 7319–7328.
- 19 B. Lu, Z. Zhu, B. Ma, W. Wang, R. Zhu and J. Zhang, *Small*, 2021, **17**, 2100946.
- 20 G. P. Lim, C. F. Soon, N. L. Ma, M. Morsin, N. Nayan, M. K. Ahmad and K. S. Tee, *Environ. Res.*, 2021, **201**, 111592.
- 21 J. Huang, Z. Li, Y. Mao and Z. Li, *Nano Sel.*, 2021, **2**, 1480–1508.
- 22 R. M. Ronchi, J. T. Arantes and S. F. Santos, *Ceram. Int.*, 2019, **45**, 18167–18188.
- 23 S. Sezen, A. Zarepour, A. Zarrabi and S. Iravani, *Microchem. J.*, 2023, **193**, 109258.
- 24 M. Huang, L. Wang, B. Zhao, G. Chen and R. Che, *J. Mater. Sci. Technol.*, 2023, **138**, 149–156.
- 25 X. Xie and N. Zhang, *Adv. Funct. Mater.*, 2020, **30**, 2002528.
- 26 M. Khazaei, A. Ranjbar, M. Arai, T. Sasaki and S. Yunoki, *J. Mater. Chem. C*, 2017, **5**, 2488–2503.
- 27 Y. Wang, Y. Xu, M. Hu, H. Ling and X. Zhu, *Nanophotonics*, 2020, **9**, 1601–1620.
- 28 S. Iravani, *Ceram. Int.*, 2022, **48**, 24144–24156.
- 29 S. Iravani and R. S. Varma, *Mater. Adv.*, 2021, **2**, 2906–2917.
- 30 S. Iravani and R. S. Varma, *Chem. Commun.*, 2022, **58**, 7336–7350.
- 31 Y. Yang, M. Anayee, A. Pattammattel, M. Shekhirev, R. J. Wang, X. Huang, Y. S. Chu, Y. Gogotsi and S. J. May, *Nanoscale*, 2024, **16**, 5760–5767.
- 32 X. Jiang, A. V. Kuklin, A. Baev, Y. Ge, H. Ågren, H. Zhang and P. N. Prasad, *Phys. Rep.*, 2020, **848**, 1–58.
- 33 Q. Sun, Z. Fu and Z. Yang, *J. Magn. Magn. Mater.*, 2020, **514**, 167141.
- 34 A. Hojjati-Najafabadi, M. Mansoorianfar, T. Liang, K. Shahin, Y. Wen, A. Bahrami, C. Karaman, N. Zare, H. Karimi-Maleh and Y. Vasseghian, *J. Water Proc. Eng.*, 2022, **47**, 102696.
- 35 V. Shukla, *Mater. Adv.*, 2020, **1**, 3104–3121.
- 36 S. Hao, H. Han, Z. Yang, M. Chen, Y. Jiang, G. Lu, L. Dong, H. Wen, H. Li and J. Liu, *Nano-Micro Lett.*, 2022, **14**, 178.
- 37 F. A. Janjhi, I. Ihsanullah, M. Bilal, R. Castro-Muñoz, B. Boczkaj and F. Gallucci, *Water Resour. Ind.*, 2023, **29**, 100202.
- 38 L. Verger, V. Natsu, M. Carey and M. W. Barsoum, *Trends Chem.*, 2019, **1**, 656–669.
- 39 L. Verger, C. Xu, V. Natsu, H.-M. Cheng, W. Ren and M. W. Barsoum, *Curr. Opin. Solid State Mater. Sci.*, 2019, **23**, 149–163.
- 40 X. He, S. Koo, E. Obeng, A. Sharma, J. Shen and J. S. Kim, *Coord. Chem. Rev.*, 2023, **492**, 215275.
- 41 F. Seidi, A. A. Shamsabadi, M. D. Firouzjaei, M. Elliott, M. R. Saeb, Y. Huang, C. Li, H. Xiao and B. Anasori, *Small*, 2023, **19**, 2206716.
- 42 S. Iravani and R. S. Varma, *RSC Adv.*, 2023, **13**, 9665–9677.
- 43 A. A. Shamsabadi, M. Sharifian Gh, B. Anasori and M. Soroush, *ACS Sustainable Chem. Eng.*, 2018, **6**, 16586–16596.
- 44 C. Dunnill, T. Patton, J. Brennan, J. Barrett, M. Dryden, J. Cooke, D. Leaper and N. T. Georgopoulos, *Int. Wound J.*, 2017, **14**, 89–96.
- 45 F. Seidi, A. Arabi Shamsabadi, M. Dadashi Firouzjaei, M. Elliott, M. R. Saeb, Y. Huang, C. Li, H. Xiao and B. Anasori, *Small*, 2023, **19**, 2206716.
- 46 K. Salimiyan rizi, *J. Mol. Struct.*, 2022, **1262**, 132958.
- 47 K. Rasool, M. Helal, A. Ali, C. E. Ren, Y. Gogotsi and K. A. Mahmoud, *ACS Nano*, 2016, **10**, 3674–3684.
- 48 H. Lin, Y. Chen and J. Shi, *Adv. Sci.*, 2018, **5**, 1800518.
- 49 M. S. Salmi, U. Ahmed, N. Aslfattahi, S. Rahman, J. G. Hardy and A. Anwar, *RSC Adv.*, 2022, **12**, 33142–33155.
- 50 S. S. Sana, M. Santhamoorthy, R. Haldar, C. J. Raorane, S. Iravani, R. S. Varma and S. C. Kim, *Process Biochem.*, 2023, **132**, 200–220.
- 51 O. S. Lee, M. E. Madjet and K. A. Mahmoud, *Nano Lett.*, 2021, **21**, 8510–8517.
- 52 X. Santos, M. Álvarez, D. Videira-Quintela, A. Mediero, J. Rodríguez, F. Guillén, J. Pozuelo and O. Martín, *Membranes*, 2022, **12**, 1146.
- 53 Q. He, H. Hu, J. Han and Z. Zhao, *Mater. Lett.*, 2022, **308**, 131100.
- 54 D. Liu, Y. Gao, Y. Song, H. Zhu, L. Zhang, Y. Xie, H. Shi, Z. Shi, Q. Yang and C. Xiong, *Biomacromolecules*, 2022, **23**, 182–195.
- 55 I. A. Alsafari, S. Munir, S. Zulfiqar, M. S. Saif, M. F. Warsi and M. Shahid, *Ceram. Int.*, 2021, **47**, 28874–28883.
- 56 L. Chen, M. Wakeel, T. Ul Haq, N. S. Alharbi, C. Chen and X. Ren, *Environ. Sci.: Nano*, 2022, **9**, 3168–3205.
- 57 A. Koyappayil, S. G. Chavan, Y. G. Roh and M. H. Lee, *Biosensors*, 2022, **12**, 454.
- 58 A. Zarepour, S. Ahmadi, N. Rabiee, A. Zarrabi and S. Iravani, *Nano-Micro Lett.*, 2023, **15**, 100.
- 59 S. M. George and B. Kandasubramanian, *Ceram. Int.*, 2020, **46**, 8522–8535.
- 60 Z. Zhang, Z. Qi, W. Kong, R. Zhang and C. Yao, *Front. Bioeng. Biotechnol.*, 2023, **11**, 1154301.
- 61 S. Song, X. Jiang, H. Shen, W. Wu, Q. Shi, M. Wan, J. Zhang, H. Mo and J. Shen, *ACS Appl. Bio Mater.*, 2021, **4**, 6912–6923.
- 62 P. O. Persson and J. Rosen, *Curr. Opin. Solid State Mater. Sci.*, 2019, **23**, 100774.
- 63 A. Liu, Y. Liu, G. Liu, A. Zhang, Y. Cheng, Y. Li, L. Zhang, L. Wang, H. Zhou and J. Liu, *Chem. Eng. J.*, 2022, **448**, 137691.



- 64 W.-J. Zhang, S. Li, V. Vijayan, J. S. Lee, S. S. Park, X. Cui, I. Chung, J. Lee, S.-k. Ahn and J. R. Kim, *Nanomaterials*, 2022, **12**, 4392.
- 65 L. Chen, X. Dai, W. Feng and Y. Chen, *Acc. Mater. Res.*, 2022, **3**, 785–798.
- 66 F. Damiri, M. H. Rahman, M. Zehravi, A. A. Awaji, M. Z. Nasrullah, H. A. Gad, M. Z. Bani-Fwaz, R. S. Varma, M. O. Germoush and H. S. Al-Malky, *Materials*, 2022, **15**, 1666.
- 67 Y. Z. Zhang, J. K. El-Demellawi, Q. Jiang, G. Ge, H. Liang, K. Lee, X. Dong and H. N. Alshareef, *Chem. Soc. Rev.*, 2020, **49**, 7229–7251.
- 68 X. Yang, C. Zhang, D. Deng, Y. Gu, H. Wang and Q. Zhong, *Small*, 2022, **18**, 2104368.
- 69 L. Mao, S. Hu, Y. Gao, L. Wang, W. Zhao, L. Fu, H. Cheng, L. Xia, S. Xie and W. Ye, *Adv. Healthcare Mater.*, 2020, **9**, 2000872.
- 70 S. S. Siwal, H. Kaur, G. Chauhan and V. K. Thakur, *Adv. NanoBiomed Res.*, 2023, **3**, 2200123.
- 71 X. Luo, Y. Liu, R. Qin, F. Ao, X. Wang, H. Zhang, M. Yang and X. Liu, *Appl. Mater. Today*, 2022, **29**, 101576.
- 72 X. Yang, C. Zhang, D. Deng, Y. Gu, H. Wang and Q. Zhong, *Small*, 2022, **18**, 2104368.
- 73 T. Li, J. Ma, W. Wang and B. Lei, *Adv. Healthcare Mater.*, 2023, **12**, 2201862.
- 74 S. Liu, D. Li, Y. Wang, G. Zhou, K. Ge, L. Jiang and D. Fang, *Biomater. Sci.*, 2022, **10**, 3585–3596.
- 75 P. Wang, Y. Wang, Y. Yi, Y. Gong, H. Ji, Y. Gan, F. Xie, J. Fan and X. Wang, *J. Nanobiotechnol.*, 2022, **20**, 259.
- 76 P. Pan, Q. Liu, L. Wang, C. Wang, L. Hu, Y. Jiang, Y. Deng, G. Li and J. Chen, *Adv. NanoBiomed Res.*, 2023, **3**, 2200126.
- 77 L. Sun, L. Fan, F. Bian, G. Chen, Y. Wang and Y. Zhao, *Research*, 2021, 2021, DOI: [10.34133/2021/9838490](https://doi.org/10.34133/2021/9838490).
- 78 H. Lu, W. Shao, B. Gao, S. Zheng and B. He, *Acta Biomater.*, 2023, **159**, 201–210.
- 79 Y. Cheng, M. Zhu, M. Chi, Y. Lai, B. Li, R. Qian, Z. Chen and G. Zhao, *ACS Appl. Mater. Interfaces*, 2024, **16**, 20105–20118.
- 80 V. Hada, D. Malvi, M. Mili, M. M. Khan, G. Chaturvedi, S. Hashmi, A. Srivastava and S. Verma, *Mater. Adv.*, 2022, **3**, 7445–7462.
- 81 F. Mohajer, G. M. Ziarani, A. Badiei, S. Iravani and R. S. Varma, *Nanomaterials*, 2023, **13**, 345.
- 82 M. Verdes, K. Mace, L. Margetts and S. Cartmell, *Curr. Opin. Biotechnol.*, 2022, **75**, 102710.
- 83 S. Yu, L. Chen, H. Xu, S. Long, J. Jiang, W. Wei, X. Niu and X. Li, *Front. Chem.*, 2022, **10**, 1063152.
- 84 L. Zhou, H. Zheng, Z. Liu, S. Wang, Z. Liu, F. Chen, H. Zhang, J. Kong, F. Zhou and Q. Zhang, *ACS Nano*, 2021, **15**, 2468–2480.
- 85 H. Zheng, S. Wang, F. Cheng, X. He, Z. Liu, W. Wang, L. Zhou and Q. Zhang, *Chem. Eng. J.*, 2021, **424**, 130148.
- 86 Y. Li, M. Han, Y. Cai, B. Jiang, Y. Zhang, B. Yuan, F. Zhou and C. Cao, *Biomater. Sci.*, 2022, **10**, 1068–1082.
- 87 S. Li, B. Gu, X. Li, S. Tang, L. Zheng, E. Ruiz-Hitzky, Z. Sun, C. Xu and X. Wang, *Adv. Healthcare Mater.*, 2022, **11**, 2102367.
- 88 D. Liu, S. Bi, H. Wang, J. Gu and S. Wang, *Composites, Part A*, 2024, **180**, 108065.
- 89 M. Mao, J. Kong, X. Ge, Y. Sun, H. Yu, J. Liu, W. Huang, D. Y. Wang and Y. Wang, *Chem. Eng. J.*, 2024, **482**, 148949.
- 90 E. M. Golebiewska and A. W. Poole, *Blood Rev.*, 2015, **29**, 153–162.
- 91 R. Medzhitov, *Cell*, 2010, **140**, 771–776.
- 92 T. Liao, Z. Chen, Y. Kuang, Z. Ren, W. Yu, W. Rao, L. Li, Y. Liu, Z. Xu and B. Jiang, *Acta Biomater.*, 2023, **159**, 312–323.
- 93 R. G. Rosique, M. J. Rosique and J. A. Farina Junior, *Int. J. Inflammation*, 2015, **2015**, 316235.
- 94 N. I. M. Fadilah, S. J. Phang, N. Kamaruzaman, A. Salleh, M. Zawani, A. Sanyal, M. Maarof and M. B. Fauzi, *Antioxidants*, 2023, **12**, 787.
- 95 A. Rafieerad, W. Yan, G. L. Sequiera, N. Sareen, E. Abu-El-Rub, M. Moudgil and S. Dhingra, *Adv. Healthcare Mater.*, 2019, **8**, 1900569.
- 96 T. Ozulumba, G. Ingavle, Y. Gogotsi and S. Sandeman, *Biomater. Sci.*, 2021, **9**, 1805–1815.
- 97 W. Yan, A. Rafieerad, K. N. Alagarsamy, L. R. Saleth, R. C. Arora and S. Dhingra, *Nano Today*, 2023, **48**, 101706.
- 98 S. M. Chin, G. Reina, N. D. Q. Chau, T. Chabrol, D. Wion, A. Bouamrani, E. Gay, Y. Nishina, A. Bianco and F. J. S. Berger, *Small*, 2023, **19**, 2208227.
- 99 J. Chen, W. Fu, F.-L. Jiang, Y. Liu and P. Jiang, *J. Mater. Chem. B*, 2023, **11**, 702–715.
- 100 S. Jiang, D. Hu, Z. Qi, L. Wang and Y. Li, *ACS Appl. Nano Mater.*, 2023, **6**, 3121–3127.
- 101 P. A. Rasheed, R. P. Pandey, F. Banat and S. W. Hasan, *Matter*, 2022, **5**, 546–572.
- 102 C. Wei, P. Tang, Y. Tang, L. Liu, X. Lu, K. Yang, Q. Wang, W. Feng, Q. T. Shubhra and Z. Wang, *Adv. Healthcare Mater.*, 2022, **11**, 2200717.
- 103 J. Chen, Y. Liu, G. Cheng, J. Guo, S. Du, J. Qiu, C. Wang, C. Li, X. Yang and T. Chen, *Small*, 2022, **18**, 2201300.
- 104 Y. Li, R. Fu, Z. Duan, C. Zhu and D. Fan, *ACS Nano*, 2022, **16**, 7486–7502.
- 105 X. Qiu, L. Nie, P. Liu, X. Xiong, F. Chen, X. Liu, P. Bu, B. Zhou, M. Tan, F. Zhan, X. Xiao, Q. Feng and K. Cai, *Biomaterials*, 2024, **308**, 122548.
- 106 R. Li, L. Zhang, L. Shi and P. Wang, *ACS Nano*, 2017, **11**, 3752–3759.
- 107 J. Meng, Z. An, Y. Liu, X. Sun and J. Li, *J. Phys. D: Appl. Phys.*, 2022, **55**, 374003.
- 108 Z. Huang, X. Cui, S. Li, J. Wei, P. Li, Y. Wang and C.-S. Lee, *Nanophotonics*, 2020, **9**, 2233–2249.
- 109 L. Jin, X. Guo, D. Gao, C. Wu, B. Hu, G. Tan, N. Du, X. Cai, Z. Yang and X. Zhang, *NPG Asia Mater.*, 2021, **13**, 24.
- 110 T. Wang, F. Rong, Y. Tang, M. Li, T. Feng, Q. Zhou, P. Li and W. Huang, *Prog. Polym. Sci.*, 2021, **116**, 101389.
- 111 L. Wang, L. Du, M. Wang, X. Wang, S. Tian, Y. Chen, X. Wang, J. Zhang, J. Nie and G. Ma, *Carbohydr. Polym.*, 2022, **285**, 119209.
- 112 X. Zhang, B. Tan, Y. Wu, M. Zhang and J. Liao, *Polymers*, 2021, **13**, 2100.



- 113 R. Luo, F. Li, Y. Wang, H. Zou, J. Shang, Y. Fan, H. Liu, Z. Xu, R. Li and H. Liu, *Mater. Des.*, 2023, **227**, 111731.
- 114 X. Han, J. Huang, H. Lin, Z. Wang, P. Li and Y. Chen, *Adv. Healthcare Mater.*, 2018, **7**, 1701394.
- 115 H. Li, R. Fan, B. Zou, J. Yan, Q. Shi and G. Guo, *J. Nanobiotechnol.*, 2023, **21**, 1–39.
- 116 C. Guo, F. Cheng, G. Liang, S. Zhang, S. Duan, Y. Fu, F. Marchetti, Z. Zhang and M. Du, *Adv. NanoBiomed Res.*, 2022, **2**, 2200064.
- 117 E. Rodriguez-Merchan, *Haemophilia*, 2012, **18**, 487–490.
- 118 Y. Yang, K. Li, Y. Wang, Z. Wu, T. P. Russell and S. Shi, *Nanomaterials*, 2022, **12**, 3792.
- 119 K. Ganguly, M. M. Espinal, S. D. Dutta, D. K. Patel, T. V. Patil, R. Luthfikasari and K.-T. Lim, *Int. J. Bioprint.*, 2023, **9**, 648.
- 120 C. Liu, W. Yao, M. Tian, J. Wei, Q. Song and W. Qiao, *Biomaterials*, 2018, **179**, 83–95.
- 121 I. A. Vasyukova, O. V. Zakharova, D. V. Kuznetsov and A. A. Gusev, *Nanomaterials*, 2022, **12**, 1797.
- 122 M. Tang, J. Li, Y. Wang, W. Han, S. Xu, M. Lu, W. Zhang and H. Li, *Symmetry*, 2022, **14**, 2232.
- 123 H. Li, J. Dai, X. Yi and F. Cheng, *Biomater. Adv.*, 2022, **140**, 213055.
- 124 Y. Yang, X. Zhou, Y. K. Chan, Z. Wang, L. Li, J. Li, K. Liang and Y. Deng, *Small*, 2022, **18**, 2105988.
- 125 L. Jin, X. Guo, D. Gao, Y. Liu, J. Ni, Z. Zhang, Y. Huang, G. Xu, Z. Yang and X. Zhang, *Bioact. Mater.*, 2022, **16**, 162–172.
- 126 S. Zhang, J. Ye, X. Liu, Y. Wang, C. Li, J. Fang, B. Chang, Y. Qi, Y. Li and G. Ning, *J. Colloid Interface Sci.*, 2021, **599**, 390–403.
- 127 J. Li, Z. Li, X. Liu, C. Li, Y. Zheng, K. W. K. Yeung, Z. Cui, Y. Liang, S. Zhu and W. Hu, *Nat. Commun.*, 2021, **12**, 1224.
- 128 X. Zhou, Z. Wang, Y. K. Chan, Y. Yang, Z. Jiao, L. Li, J. Li, K. Liang and Y. Deng, *Adv. Funct. Mater.*, 2022, **32**, 2109469.
- 129 Z. Yang, X. Fu, D. Ma, Y. Wang, L. Peng, J. Shi, J. Sun, X. Gan, Y. Deng and W. Yang, *Small*, 2021, **17**, 2103993.
- 130 F. Hao, L. Wang, B. Chen, L. Qiu, J. Nie and G. Ma, *ACS Appl. Mater. Interfaces*, 2021, **13**, 46938–46950.
- 131 Y. Shao, K. Dong, X. Lu, B. Gao and B. He, *ACS Appl. Mater. Interfaces*, 2022, **14**, 56525–56534.
- 132 L. Jin, Y. Ma, R. Wang, S. Zhao, Z. Ren, S. Ma, Y. Shi, B. Hu and Y. Guo, *Mater. Today Adv.*, 2022, **14**, 100224.
- 133 T. Liu, Y. Lu, R. Zhan, W. Qian and G. Luo, *Adv. Drug Delivery Rev.*, 2022, **193**, 114670.
- 134 C. E. Shuck, A. Sarycheva, M. Anayee, A. Levitt, Y. Zhu, S. Uzun, V. Balitskiy, V. Zahorodna, O. Gogotsi and Y. Gogotsi, *Adv. Eng. Mater.*, 2020, **22**, 1901241.
- 135 W. Eom, H. Shin, R. B. Ambade, S. H. Lee, K. H. Lee, D. J. Kang and T. H. Han, *Nat. Commun.*, 2020, **11**, 2825.
- 136 S. Jolly, M. P. Paranthaman and M. Naguib, *Mater. Today Adv.*, 2021, **10**, 100139.
- 137 N. J. Prakash and B. Kandasubramanian, *J. Alloys Compd.*, 2021, **862**, 158547.
- 138 G. Murali, J. K. Reddy Modigunta, Y. H. Park, J. H. Lee, J. Rawal, S. Y. Lee, I. In and S. J. Park, *ACS Nano*, 2022, **16**, 13370–13429.
- 139 J. Jiang, S. Bai, J. Zou, S. Liu, J. P. Hsu, N. Li, G. Zhu, Z. Zhuang, Q. Kang and Y. Zhang, *Nano Res.*, 2022, **15**, 6551–6567.
- 140 S. Iravani, *Ceram. Int.*, 2022, **48**, 24144–24156.
- 141 K. Velusamy, P. Chellam, P. S. Kumar, J. Venkatachalam, S. Periyasamy and R. Saravanan, *Environ. Pollut.*, 2022, **301**, 119034.
- 142 J. A. Kumar, P. Prakash, T. Krithiga, D. J. Amarnath, J. Premkumar, N. Rajamohan, Y. Vasseghian, P. Saravanan and M. Rajasimman, *Chemosphere*, 2022, **286**, 131607.
- 143 X. Lin, Z. Li, J. Qiu, Q. Wang, J. Wang, H. Zhang and T. Chen, *Biomater. Sci.*, 2021, **9**, 5437–5471.
- 144 Y. Wang, W. Feng and Y. Chen, *Chin. Chem. Lett.*, 2020, **31**, 937–946.
- 145 E. Mostafavi and S. Iravani, *Nano-Micro Lett.*, 2022, **14**, 130.
- 146 M. Khatami, P. Iravani, G. Jamalipour Soufi and S. Iravani, *Mater. Technol.*, 2022, **37**, 1890–1905.
- 147 K. Zheng, S. Li, L. Jing, P. Y. Chen and J. Xie, *Adv. Healthcare Mater.*, 2020, **9**, 2001007.
- 148 A. Szuplewska, D. Kulpińska, A. Dybko, M. Chudy, A. M. Jastrzębska, A. Olszyna and Z. Brzózka, *Trends Biotechnol.*, 2020, **38**, 264–279.
- 149 R. Manisekaran, A.-D. R. Chettiar, G. Kandasamy, R. Garcia-Contreras and L. S. Acosta-Torres, *Biomater. Adv.*, 2023, **147**, 213354.
- 150 C. Dai, H. Lin, G. Xu, Z. Liu, R. Wu and Y. Chen, *Chem. Mater.*, 2017, **29**, 8637–8652.
- 151 Y. Xu, Y. Wang, J. An, A. C. Sedgwick, M. Li, J. Xie, W. Hu, J. Kang, S. Sen and A. Steinbrueck, *Bioact. Mater.*, 2022, **14**, 76–85.
- 152 K. Chaturvedi, V. Hada, S. Paul, B. Sarma, D. Malvi, M. Dhangar, H. Bajpai, A. Singhane, A. K. Srivastava and S. Verma, *Top. Curr. Chem.*, 2023, **381**, 11.

